首都圏におけるやや深い構造の地震波速度

著者	山水 史生
雑誌名	防災科学技術研究所　研究報告
巻	56
ページ	1-32
発行年	1996-02
URL	http://doi.org/10.24732/nied.00001070

Report of the National Research Institute for Earth Science and Disaster Prevention, No, 56 ; February, 1996

Down-Hole Measurements of Seismic Wave Velocities in Deep Soil Deposits beneath the Tokyo Metropolitan Area

By

Fumio YAMAMIZU*

National Research Institute for Earth Science and Disaster Prevention, Japan

Abstract

From both the seismological and earthquake engineering points of view, deep seismic P and S wave velocities were directly and systematically measured down to the depth of 2 to 3 km at the three deep borehole observatories of Iwatsuki, Shimohsa, and Fuchu which were constructed for geophysical observations in the Tokyo metropolitan area. The measurement was focused on the S wave velocity rather than the P wave velocity because the S wave velocity is more important for the earthquake resistant problems. In the measurements, we adopted the down-hole method in which the seismic waves from the surface source are detected by a three component down-hole receiver. S waves were excited by two types of sources ; one is an ordinary small explosion of dynamite and the other is a specially designed gun-type SH wave generator. For each site, the number of measured depths was 15-17, and short intervals (100m) were chosen in shallower positions, but longer intervals (250-500m) were chosen in deeper depths.

Present measurements revealed that the underground structure beneath the three sites is fundamentally composed of two layers which cover the basement rocks. S wave velocities, without a distinction between the three sites, are 0.4-0.9km/sec for the uppermost Pleistocene soils, 1.2-1.9km/sec for the middle Miocene layers, and 2.5-2.6km/sec for the pre-Neogene or pre-Tertiary basement, and those of the P wave are 1.8-2.1km/sec, 2.4-3.2km/sec, and 4.7-5.0km/sec, respectively. A common feature of the underground sturcture at the three sites is a similar thickness (about 1.0km) of the Pleistocene soils, notwithstanding differences of the basement depth. It was also revealed that the velocity of the basement rocks is systematically different both for S and P waves between the present results and the refraction surveys by the Yumenoshima explosion. This fact suggests that the basement structure is not simple and uniform but complex and irregular. Finally, the gross feature of the 3-D structure beneath the Tokyo metropolitan area is figured by summarizing the present results, the geological data of other boreholes, and results of various seismic refraction surveys in and around the Tokyo metropolitan area.

Key words : Borehole Observatory, Deep Soil Deposit, Down-Hole Method, P Wave Velocity, S Wave Velocity, Velocity Structure.

Contents

* Advanced Measurement and Analysis Technology Division. Computational Sciences Laboratory.

1. Introduction

1.1 Significance of the Down-Hole Measurements

The Tokyo metropolitan area is widely covered by soft and thick sedimentary layers to a depth of several kilometers. To elucidate the velocity structure of such a thick sediment and the basement rock is of fundamental significance in both fields of seismology and earthquake engineering. The seismic source process, which is one of the most important problems in seismology, is precisely evaluated after effects of thick sedimentary layers upon the seismic wave propagation are eliminated (Helmberger and Johnson, 1977 ; Bouchon, 1979). And, various theoretical studies on the generation of the strong ground motion have taken the dynamical characteristics of thick sediment into consideration (Heaton and Helmberger, 1977, 1978 ; Archuleta and Day, 1977 ; Bouchon and Aki, 1980 ; Aki, 1982). In the field of earthquake engineering, thick sedimentary layers have become an essential problem for the antiseismic design of large-scale structures, such as high-rise buildings, suspension bridges, oil tanks, and reservoirs. This is because these structures have a rather long fundamental period of 5-10sec and this rather long period of motion is closely related to the velocity structure of thick sediment (Kanamori, 1974 ; Butler and Kanamori, 1980). Also, the seismic zoning map, which estimates the seismic intensity of the ground surface for future earthquakes, is drawn up on the basis of the physical properties of the sediment.

Among the physical parameters, such as the seismic P and S wave velocities, the medium density, and other anelastic properties of the formation of sedimentary layers, the S wave velocity is the most important and indispensable. The best method that provides not only the S wave but also the P wave velocity of sediments is the direct measurement in deep holes by logging or the down-hole method. P wave velocities, from the view point of oil-exploration or mineral-prospecting, were precisely investigated by means of logging as deep as several kilometers in many places throughout the world. However, for S wave velocities, which are more important in geophysics and engineering, the logging depths have been limited to at most 100-200 meters due to difficulties in the experiments.

The measurement of the S wave velocity by means of logging was started in the 1950's by Jolly (1956) and Macdonal *et al.* (1958). The measurement process progressed in the USA by White and Sengbush (1963), and in Russia (USSR) by Kovalev and Molotova (1960), and Halperin and Frolova (1961). White (1965), in publishing a textbook on borehole elastic wave measurement, marked a new epoch. Slightly later, Kitsunezaki (1967) and Ohta (1968) began work in this field which paved the way in Japan for S wave velocity logging. Subsequent studies in Japan and around the world are summarized by Kitsunezaki (1976) and Murphy (1978), respectively. In those studies, however, the effort was devoted to near-surface soils at a depth of less than 200 meters, except for some trial measurements. One of the exceptions is the experiment by Erickson *et al.* (1968), in which travel-time curves were drawn as deep as 1700 meters. More recently, the logging depth was extended to about one kilometer by Lash (1980) and Stewart *et al.* (1981) for studying the subsurface fracture zone by vertical seismic profiling. Kitsunezaki (1980) designed a new instrument for S wave logging, the suspension-type sonde system. This sonde system is composed of an indirect-excitation type source and suspension-type receivers. The system was developed in response to requirements for S wave measurements deeper than the earlier ones with easier operation and higher reliability. But the sonde system has not been applied to the measurement deeper than several kilometers in practice.

The needs of seismology and earthquake engineering motivated us to elucidate not only the S wave but also the P wave characteristics of thick sedimentary strata down to at least several kilometers. In line with these scientific needs, at first, the seismic wave velocity logging by means of the down-hole method which focused on the S wave velocity rather than the P wave velocity was planned and carried out down to 2 to 3km in depth by using the three deep holes at Iwatsuki, Shimohsa, and Fuchu. These three deep holes were constructed by the National Research Institute for Earth Science and Disaster Prevention

(NIED) for geophysical observations in the Tokyo metropolitan area as a part of the national program of earthquake prediction (Takahashi and Hamada, 1975 ; Hamada *et al.*, 1978).

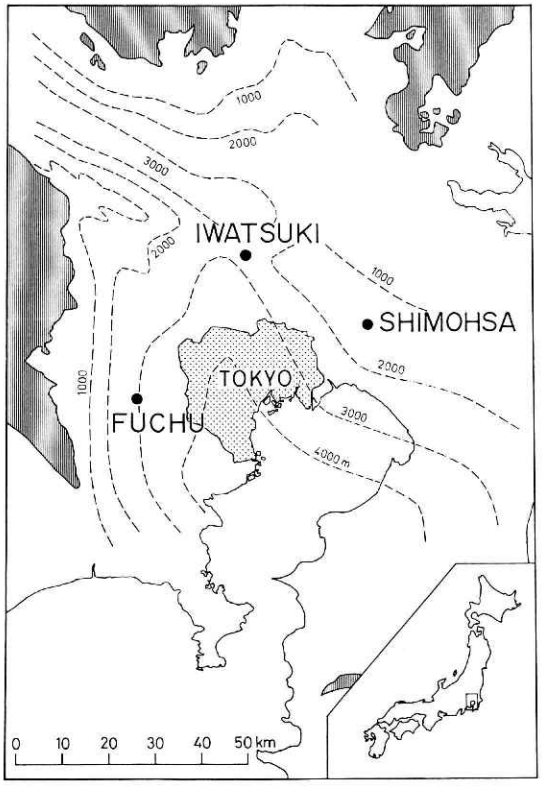

Fig. 1 Location of the Deep Borehole Crustal Activity Observatories of NIED. The shaded area and dashed contours represent the outcrop and the depth (meter) of the pre-Neogene basement rocks, respectively (after Kakimi *et al.*, 1973).

1.2 Observation Holes

The three deep borehole observatories at Iwatsuki, Shimohsa, and Fuchu were constructed by 1980, and they are now in routine operation. These boreholes are located just around the Tokyo metropolitan area, where thick sedimentary layers are deposited down to about 4 kilometers at most (Kakimi *et al.*, 1973) as shown in Fig. 1. All of the boreholes pierce through the sedimentary layers of the Pleistocene and Miocene, and penetrate into the pre-Tertiary or pre-Neogene basement which is composed of metamorphic or crystalline rocks. The depth to the basement is between 1.5-3.0km, though it differs from site to site. The geographical position and the depth of the holes are summarized in Table 1.

The hole structures are schematically shown in Fig. 2 (Takahashi, 1982). The holes are cased by multiple steel pipes, which are firmly adhered to the rock wall by expansion cement and are filled with rustproof water. The hole axis is held strictly vertical ; the deflection from the vertical is within only 3 degrees from the top to the bottom. The effective diameter of the hole at Iwatsuki is constant at 15.9cm from the top to the bottom. At both Shimohsa and Fuchu, the diameter changes from 22.7cm in the shallower area to 15.5cm in the deeper area. The depth for this change is at about 1.3km at Shimohsa and 1.9km at Fuchu. A plug-type noise shutter is put into this step-like structure for removing undesirable ground noises which are excited on the ground surface and trapped in the hole water (Yamamoto *et al.*, 1975 ; Yamamizu *et al.*, 1977 ; Yamamizu, 1980). In the holes, the temperature monotonically increases with

Table 1 Geographical position and depth of the deep holes at the Iwatsuki, Shimohsa, and Fuchu Observatories.

	Iwatsuki	Shimohsa	Fuchu
Address	2,878-1 Makinoue Sueda Iwatsuki-shi Saitama-ken	1,293 Fujigaya Shonan-machi Chiba-ken	6-65 Minami-machi Fuchu-shi Tokyo
Longitude (E)	139°44′17.0″	140° 1′25.6″	139°28′25.1″
Latitude (N)	35°55′33.0″	35°47′36.4″	35°39′ 2.4″
Altitude (meter)	8.96	22.81	44.71
Bottom depth (meter)	3,510	2,300	2,750

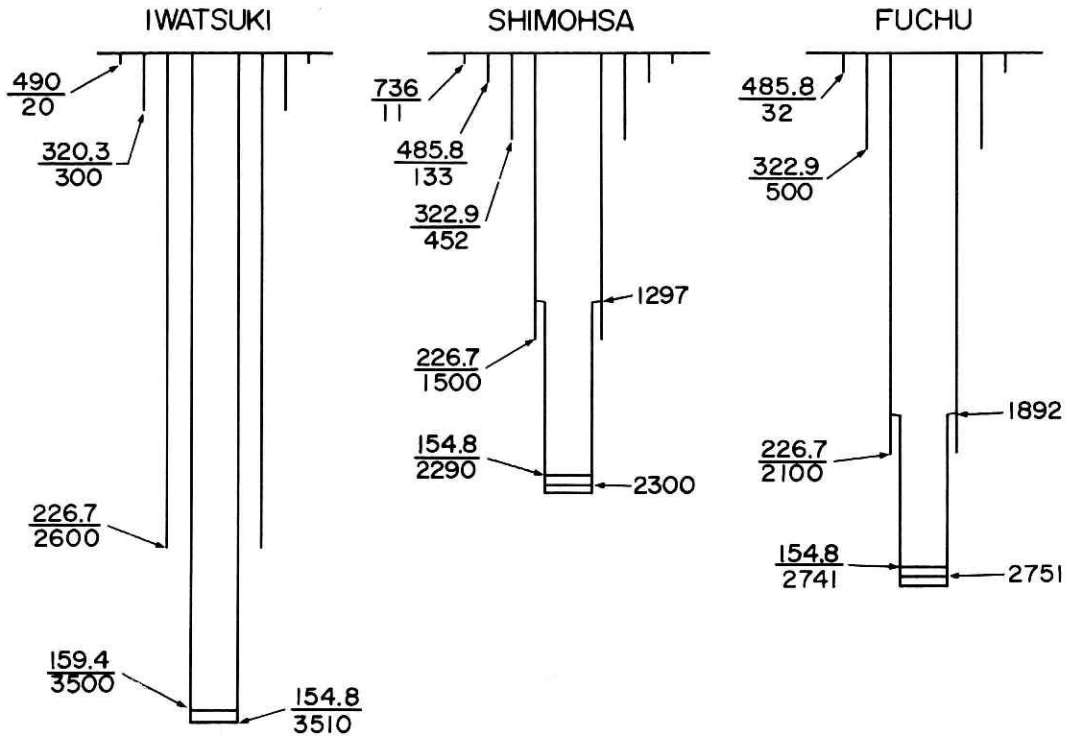

Fig. 2 Structure of the three deep holes of Iwatsuki, Shimohsa, and Fuchu with the inner diameter (cm, upper figure) and depth (m, lower figure) of the casings.

depth, and the temperature at the bottom is 86°C, 61°C, and 78°C at Iwatsuki, Shimohsa, and Fuchu, respectively. Details of the observation holes and instruments for the geophysical observations are described in Takahashi and Hamada (1975), Hamada *et al.* (1978), and Takahashi (1982).

1.3 Framework of Measurements

The experiment was carried out based on the down-hole method as schematically shown in Fig. 3. The down-hole technique uses a surface source and a down-hole receiver. The receiver is fixed at the desired depth in the hole and the waves from the source are recorded. The receiver is then moved to an other depth where the measurement is repeated. The biggest problems that potentially restrict the down-hole technique are the lack of source power and troubles in the operation of the receivers. These weak points were overcome by using special sources and a special receiver as described in the following.

For S wave generation, two types of sources were introduced. One is the simple detonation of a small charge of dynamite (0.1-5kg) in a subsidiary shallow hole, the shot-hole, with a depth of 10-20 meters. The detonation source produces a non-polarized SV wave rather than a polarized SH wave, although those waves are contaminated by a predominant precursory P wave. The other source is a gun-type SH wave

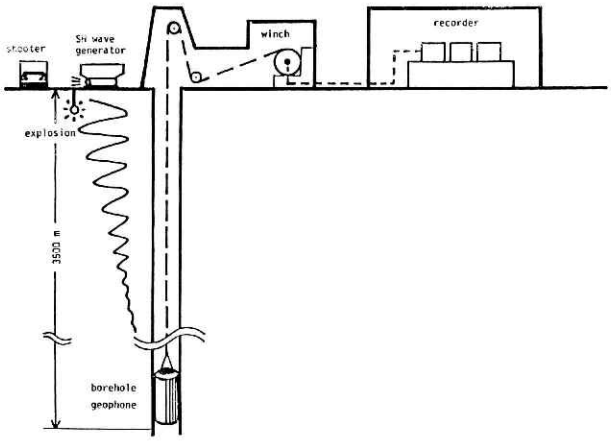

Fig. 3 Schematic representation of the down-hole method.

generator, so called the S gun, which was proposed and designed by Shima and Ohta (1968) about 25 years ago. The use of polarized SH waves greatly facilitates the identification of the first arrival of the S wave. As is described later, the validity of the S gun for generating the SH wave had been demonstrated by experiments at Iwatsuki and Shimohsa (Ohta *et al.*, 1977, 1978, 1980). For the experiment at Fuchu, a new S gun was designed and used (Yamamizu *et al.*, 1981a, b). This new S gun was enlarged and strengthened more than the previous one so as to improve the power and stability for the SH wave generation. The general view of the previous and new SH wave gener-

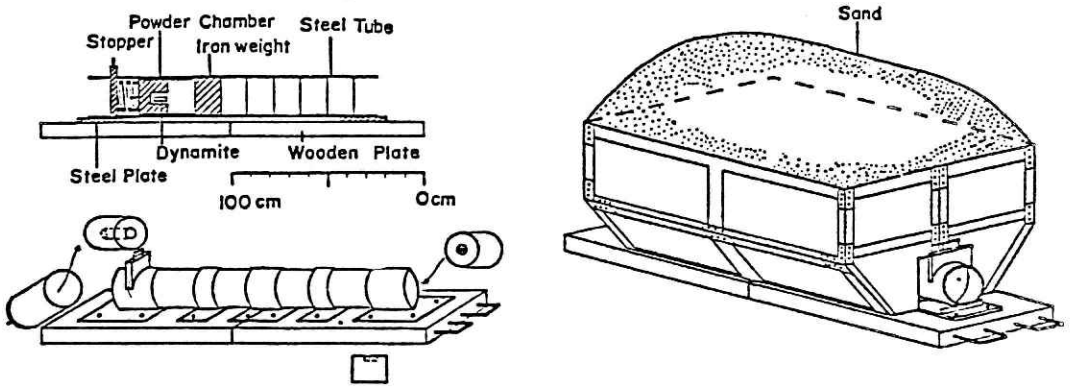

Fig. 4a General view of the SH wave generator (old type).

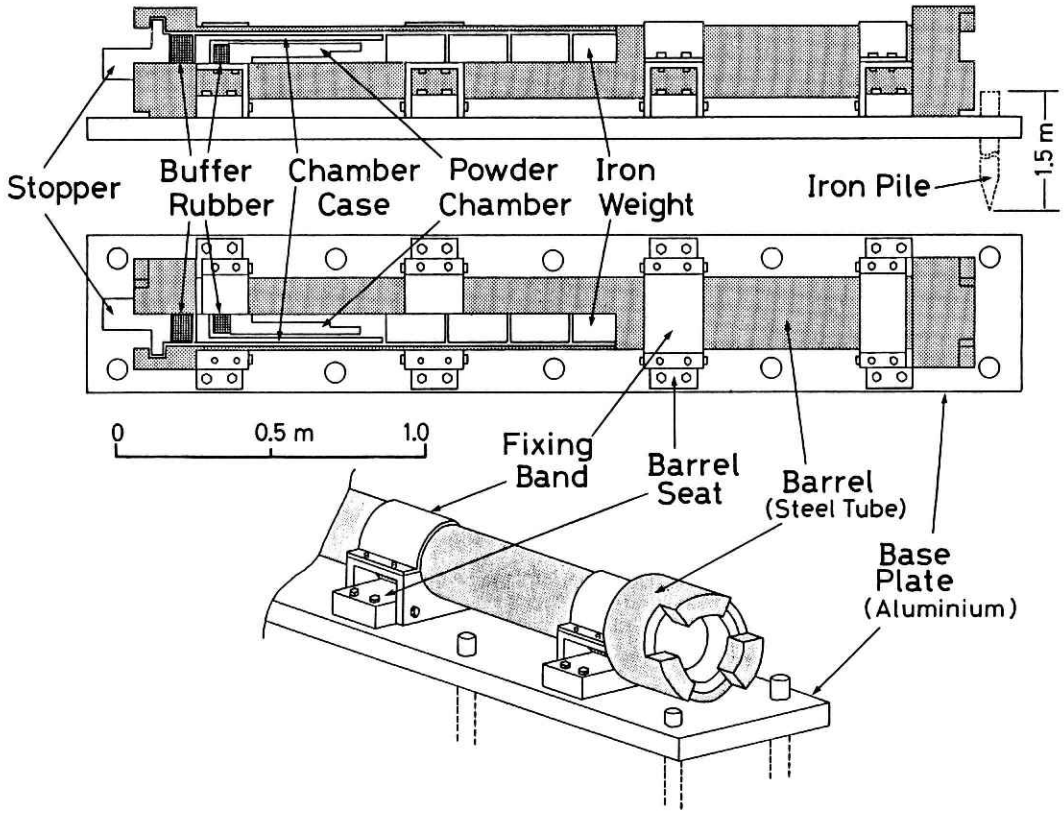

Fig. 4b General view of the SH wave generator (new production).

ators are illustrated in Fig. 4a and 4b, respectively.

The down-hole receiver, a set of three component seismometers, was installed in a specially-designed capsule with a clamping device in order to be fixed at any depth in the hole. The capsule is of the same type as is used for continuous observation under high pressure and temperature circumstances at the hole bottom. Though the constitution of the three observation systems is slightly different, the functions of the systems are basically the same; the output signal from the receiver is pre-amplified, low-pass filtered, then divided into three channels with different gains of 1 : 5 : 25 ratio to cover a wide dynamic range. All the signals are recorded on magnetic tape and are simultanuously monitored by a multi-channel pen-recorder (see Fig. 6, Fig. 14, and Fig.22).

Before the experiments, a working plan was carefully elaborated in order to efficiently perform the large-scale experiments in which many expert technicians participated. The technicians were arranged into four working parties: measurement, winch-operation, receiver-control, and source-detonation parties. In advance of the operation, the headquaters gave directives about the measuring depths and sources to all the parties. Following the headquaters directives, the receiver was moved to the depth appointed, and fixed to the hole wall by remote-control. Then, the amplifier gain and the cut-off frequency of the filter

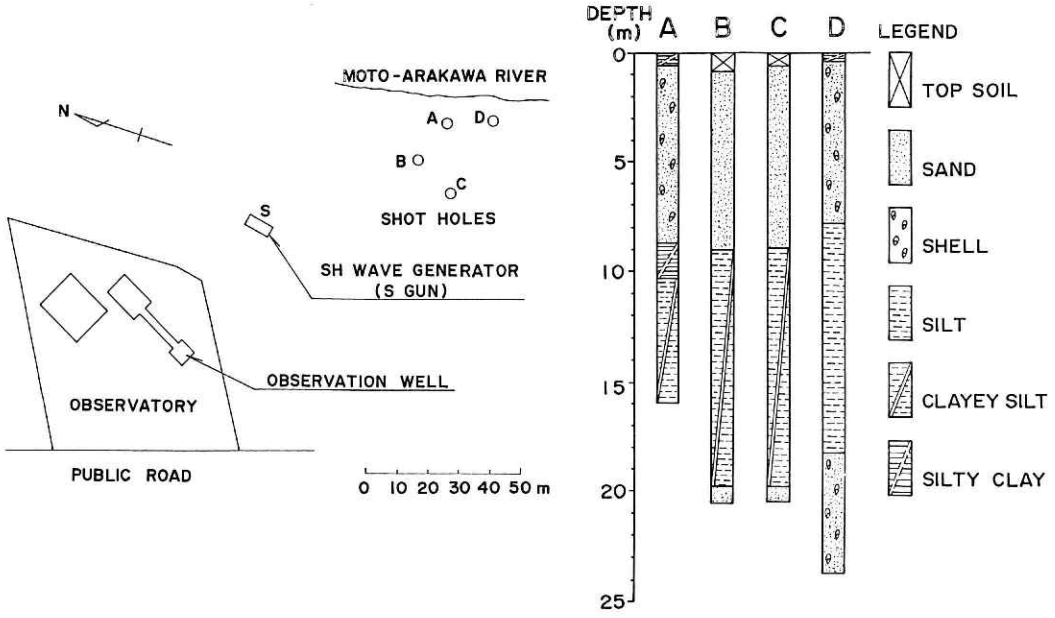

Fig. 5 Plan of the experimental field at Iwatsuki. Soil profiles of four shot-holes are shown in the right side.

were adjusted to monitor the ground noise. On the other hand, sources were prepared at the same time ; the SH wave generator and shot-holes were charged with black powder and dynamite, respectively. Second, after the preparation stage, the measurement party decided the ignition timing of the source keeping close contact with the source-detonation party for the sake of the safety around the source. Thus, several measurements were done at the same depth. Third, the measurement party confirmed the quality of the records from several source blasts, then reported a completion of measurements at that depth to the headquaters. Finally, the headquaters announced to all the parties that the measurements at that particular depth were finished. In this way, the experimental process was cyclically repeated. The depth interval for the measurement was chosen to be short in length (100m) in shallower depths, but longer (250-300m) in deeper depths. This is because the soil condition is more complex in shallower area, while it becomes more stable in deeper area.

2. Measurement at Iwatsuki

2.1 Experiment

The first experimental site, the Iwatsuki Deep Borehole Observatory at Iwatsuki City, Saitama Prefecture, is located about 30km north of central Tokyo. According to the geological columnar section examined when drilling the Iwatsuki borehole, the younger soil deposits reach 2.8km in depth, overlaying the pre-Tertiary basement rock (Chichibu crystalline rock system). The depth of the hole bottom is 3.5km (Fig. 2).

Needless to say, the SH wave generator is much better for identification of the S wave arrival than the simple explosion source. But, at the time the measurement was planed, there was no experience in how deep the S wave signal could be detected by using the S gun. Therefore, ordinary simple detonation in a subsidiary shallow hole (10-20m in depth) was mainly used, and the S gun was only used as a supplement. The maximum charge we could put into the powder chamber of the S gun was 300gr. As shown in Fig. 5, four shot-holes were drilled about 100m southeast of the observation hole for the ordinary detonation, and the S gun was firmly fixed on the ground surface about 50m east of the observation hole. The profiles of the soil conditions of the shot-holes are also shown in the same figure.

The block diagram of the total observation system is shown in Fig. 6. The natural frequency of a three-component seismometer is 4.5 Hz. The signals from those seismometers were recorded on 30-min compact cassette tapes by three data recorders with high, medium, and low gains. The ignition signal was also recorded on the individual channel of each data recorder on which a 50 Hz clock signal was convoluted. Another set of the three-component seismometer was operated on the ground surface in order to check the S wave generation of the source.

Experiments were conducted at 16 different depths ;

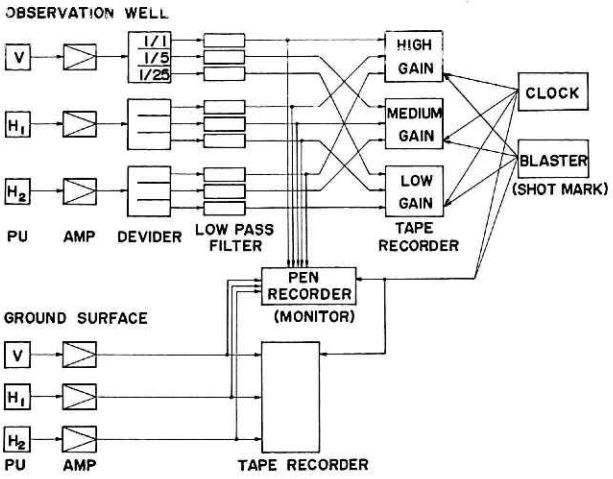

Fig. 6 Block diagram of the observation system for the measurement at Iwatsuki.

that is, at 0.1, 0.2, 0.3, 0.5, 0.75, 1.0, 1.25, 1.5, 1.75, 2.0, 2.25, 2.5, 2.75, 3.0, 3.25, and 3.482km (bottom of the hole). At one depth, measurements were repeated 3 to 5 times for both types of sources, and this measurement took about 2 hours including the moving and fixing of the receiver capsule. Within the turn around time, the depth and charge size for the next measurement were decided by carefully watching and monitoring the records, and the interval velocity of the seismic waves was roughly analysed by using the records obtained from the completed measurements. The measuring conditions, depth, charge size, and source type are summarized in Table 2. The total number of blasts were 48.

2.2 Data and Analysis

Since this was the first experience of the down-hole measurement of the S wave velocity over the depths of several kilometers, the analysis proceeded by giving priority to the detection and identification of the S wave. Also, this way of analysis was inevitably required because the interval of measurements was rather rough, approximately 100-250m. All efforts were concentrated on objectively determining the S wave structure from the travel-times observed so that any other data concerning the observation hole, for example, the sonic and density logging, were not taken into account. At the last stage of analysis, the final result obtained was carefully compared with all the related data and the harmony between them was examined.

Along this line, at first, the record from the SH wave generator was processed. Figure 7 illustrates the SH waves from the S gun. All the traces in this figure are modified by using the azimuth converter which is shown in Fig. 8 as a block diagram. The direction of the horizontal receiver in the hole is not known, but through this converter the receiver direction can experimentally agree with the polarization direction of the SH waves. The effect of the azimuth converter is remarkable especially for the trace of the 1500m depth in which the SH wave is expectedly emphasized as shown in Fig. 7. The measurement by

Table 2 Specifications of the measuring conditions of the experiment at Iwatsuki.

Date Y.M.D.	Meas. Depth (km)	Type	Source Charge (gr)	Depth (m)	Date Y.M.D.	Meas. Depth (km)	Type	Source Charge (gr)	Depth (m)	Date Y.M.D.	Meas. Depth (km)	Type	Source Charge (gr)	Depth (m)
1976														
Nov. 8	0.1	S	100		Nov. 9	0.75	A	500	15.1	Nov.11	2.5	A	4000	14.1
	0.1	S	100											
	0.1	A	50	15.0		1.0	S	300			3.0	D	1000	5.0
	0.1	D	100	21.0		1.0	D	300	11.6		3.0	C	4000	20.2
						1.0	A	1000	15.1		3.0	B	4000	19.4
	0.2	S	100								3.0	A	8000	13.9
	0.2	S	100		Nov. 10	1.5	S	300						
	0.2	A	100	15.0		1.5	D	500	10.3	Nov. 12	3.48	C	2000	18.1
	0.2	D	300	15.0		1.5	A	2000	14.7		3.48	A	400	10.0
	0.3	S	200			1.25	C	1000	3.5		3.25	B	4000	18.3
	0.3	A	25	15.5		1.25	B	2000	10.2		3.25	C	5000	13.0
	0.3	D	100	14.0										
						2.0	B	50	20.1		2.75	B	4000	7.7
Nov. 9	0.5	S	200			2.0	C	200	20.5		2.75	C	5000	10.0
	0.5	D	100	13.0		2.0	D	500	7.7					
	0.5	A	300	15.5		2.0	A	2000	14.6	Nov. 13	2.25	C	1000	6.0
	0.5	S	200								2.25	B	4000	16.6
					Nov. 11	2.5	D	500	5.5					
	0.75	S	200			2.5	C	1000	20.5		1.75	A	1000	6.5
	0.75	D	200	13.5		2.5	B	2000	19.9		1.75	B	2000	12.3

Type S and A-D represent the S-gun and shot-holes, respectively.

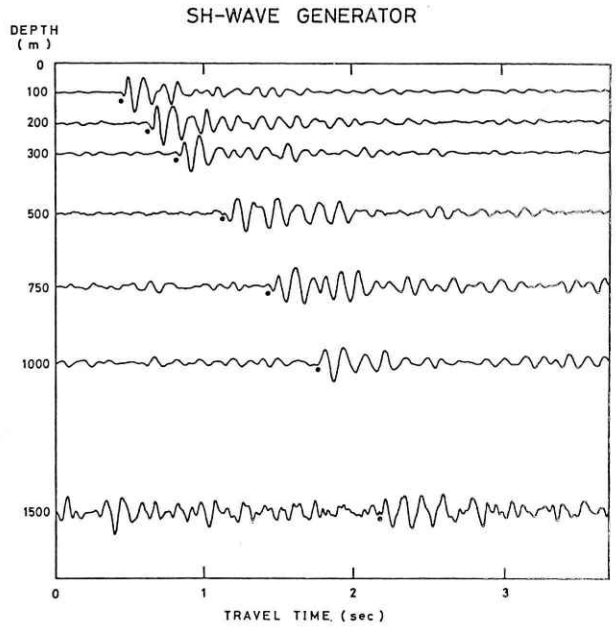

Fig. 7 Paste-up SH waves by the SH wave generator obtained in the measurement at Iwatsuki. Solid circles are the onsets of the SH waves.

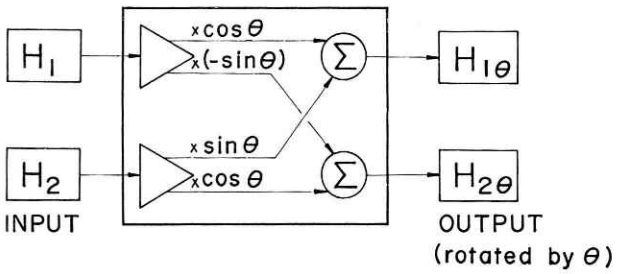

Fig. 8 Block diagram of the azimuth conversion circuit.

using the S gun was terminated at 1500m in depth since the black gun-powder charged was anticipated to exceed the maximum for keeping the S gun safe.

The complete SV wave section for the simple detonation source is presented in Fig. 9, in which horizontal component records are arranged after filtering for the most appropriate pass-band. The azimuth converter was also applied to those records, but the result was not improved. The reason is that the detonation source predominantly produces a non-polarized SV wave rather than an SH wave. Accordingly, the improvement of the waveform was primarily accomplished by frequency filtering with various pass-bands. There may be a doubt about the appropriateness of the onset positions of the S waves in Fig. 9, but these were carefully determined down to 1500m by comparing with clearer onsets by means of the S gun, and then the rest were identified by extrapolation. For identifying the S wave onset, a change of the

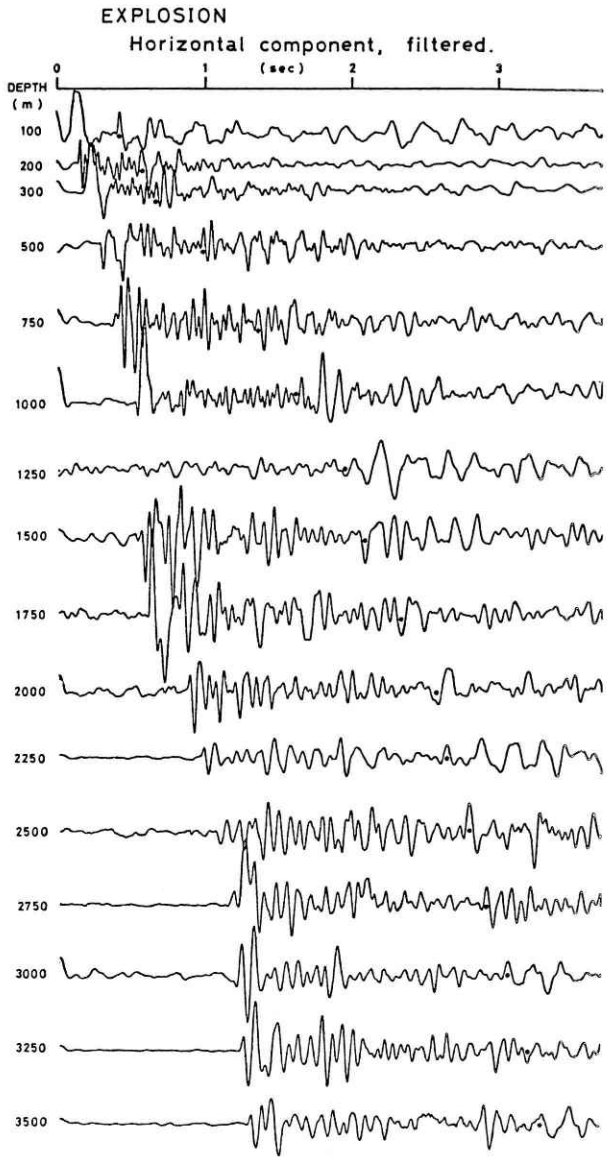

Fig. 9 Paste-up seismograms of the horizontal component by small explosions obtained in the measurement at Iwatsuki. Solid circles are the onsets of the S waves.

wave period was also useful (Kubotera and Ohta, 1967). The S wave onsets, represented by the solid circles in Fig. 9, were decided in this way.

Next, for the P wave section, a similar procedure was applied using the vertical component records from the detonation source. In this case, a simple filtering was adopted only for the purpose of decreasing undesirable noises, since the P wave arrives first and is strong enough for detection. The complete P wave section is pasted up in Fig. 10. In the figure, we see three wave groups ; the first wave group is the precursor with a small amplitude, appearing at the shallower depth down to 2500m ; the second is the true P wave group ; and the third group following the P waves has large amplitudes. Judging from a rough

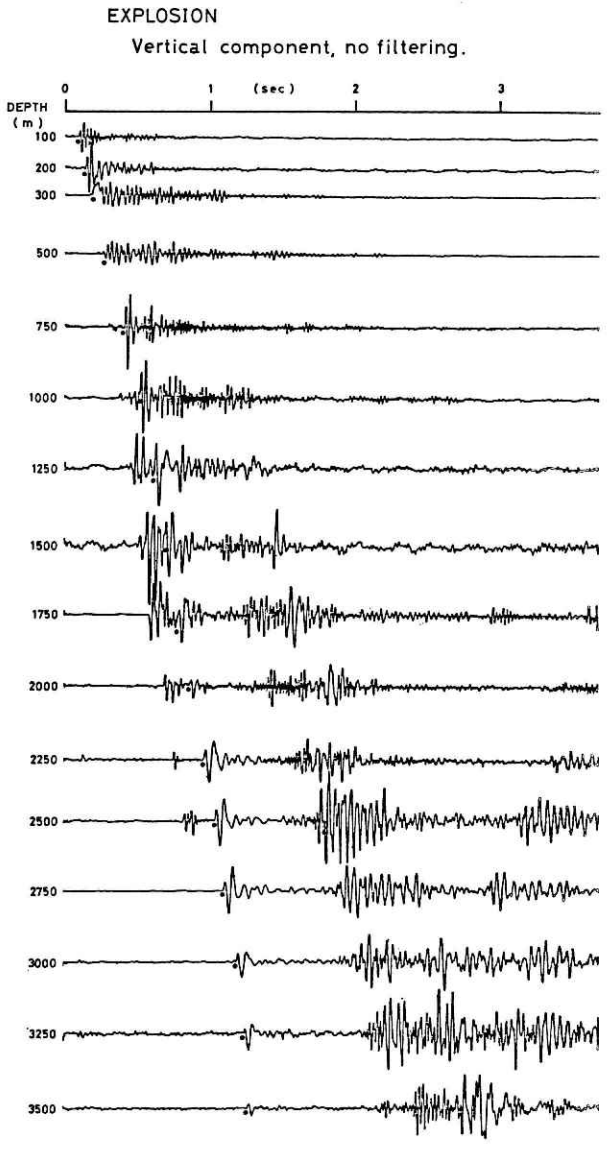

Fig. 10 Paste-up seismograms of the vertical component by small explosions obtained in the measurement at Iwatsuki. Solid circles are the onsets of the P waves.

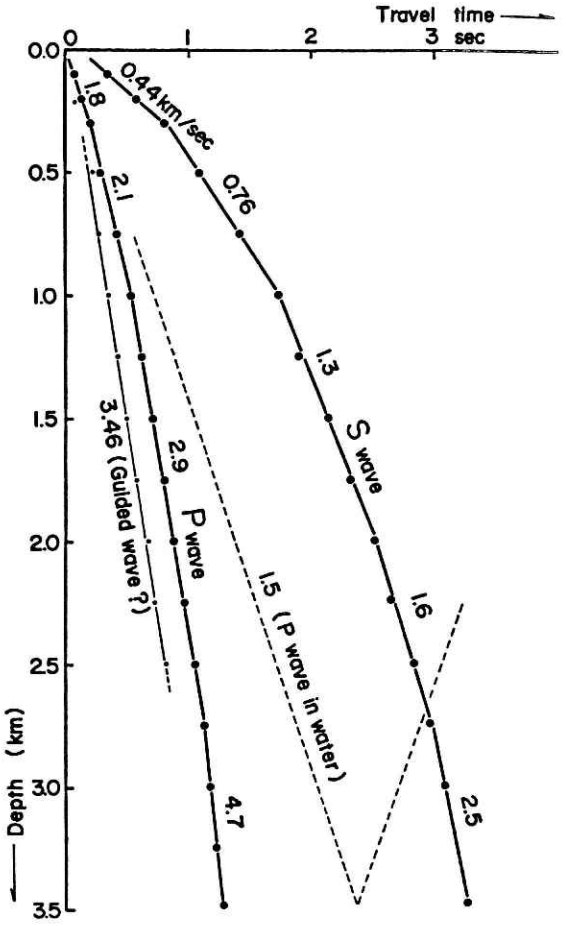

Fig. 11 Travel-time versus depth plots of S, P, and other marked wave groups for the measurement at Iwatsuki.

estimation of propagating velocities, the first and third groups are concluded to be the guided P waves which propagate through the cemented zone between the steel casing pipe and the surrounding rock and through the water filled in the hole, respectively. Especially, the third group is unquestionable because clear reflection at the bottom is recognized.

2.3 Velocity Structure

The interval velocities of S and P waves are deduced from the first-arriving S and P waves in the SH, SV, and P wave sections. The onsets of each wave were read at the precision of 0.01 second. After that, the travel-time was corrected for the imaginary source at the top of the observation hole. In the correction, we used detailed velocity structures of S and P waves to the depth of 120m which were obtained by another experiment carried out in the auxiliary hole close to the observation hole (Fig. 12). In Figure 11, the travel-times of S and P, and other phases are plotted, and the travel-time curves are drawn through the data points. All the plots, except a few points, satisfactorily match the curve with a deviation of only 0.03sec. From these curves, we can directly determine the interval velocities of the S and P waves.

The S wave velocity structure, except for in the vicinity of the ground surface, consists of four layers; and that of the P wave consists of three layers covering the deep basement. The derived S wave velocities for the four layers and the basement are 0.44, 0.76, 1.3, 1.6, and 2.5km/sec from the top to the bottom. The one way time is 3.27sec for an S wave. The velocity contrast is remarkably large at the soil-rock boundary, as was expected. The P wave velocities are, from the top to the bottom, 1.8, 2.1, 2.9, and

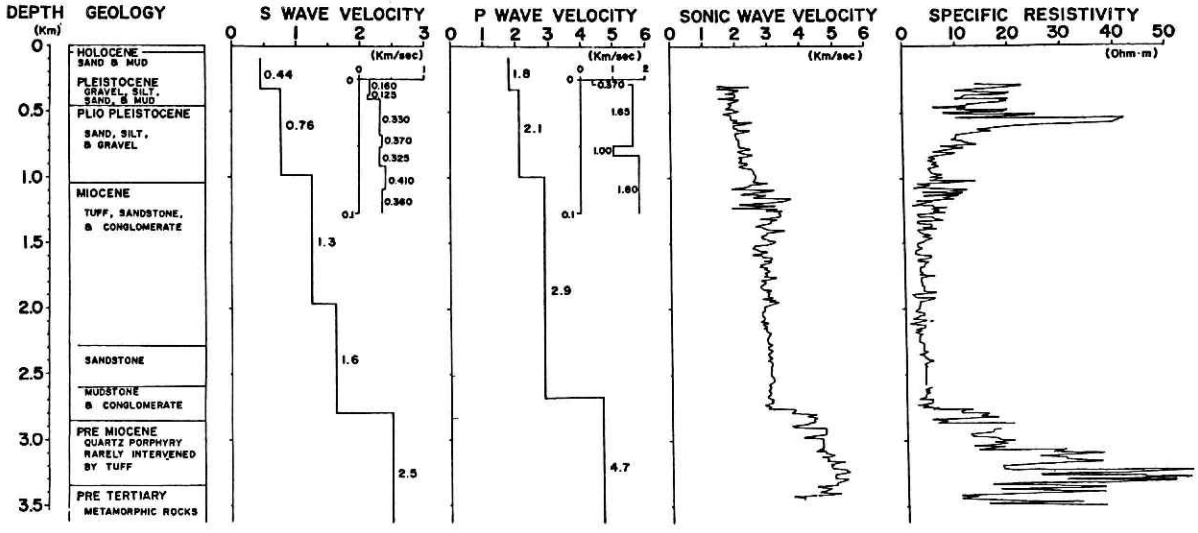

Fig. 12 S and P wave velocity structures at Iwatsuki in comparison with the geological section, sonic velocity, and electric resistivity. Subsurface (shallower than 100m) structures were obtained from a supplementary measurement by means of the conventional technique.

4.7km/sec, and all the layer-interface depths are consistent with those of the S wave. The only discrepancy is the boundary between the layers with the S velocity of 1.3 and 1.6km/sec, which appeared only for the S wave. The discontinuity in the S velocity between those layers is not sharp, so that those two layers might be taken as a single layer with a continuously increasing velocity.

The S and P wave velocity profiles are shown in Fig. 12 in comparison with other geophysical and geological data including the sonic wave velocity and electric resistivity. Mutual consistency among them is generally good. Variation of the sonic wave velocity seems very complex because the sonic logging by means of the continuous measurement can detect finer changes of velocity than the present down-hole method. But the general trend and velocity value on average are in good harmony with the P wave velocity profile obtained in the present experiment. The velocity discontinuities at the depth of 1.0 and 2.8km are clearly seen also in the sonic log profile, and those boundaries fairly well correspond to the geological profiles of the Pleistocene-Miocene and the Miocene-pre-Tertiary eras, respectively.

3. Measurement at Shimohsa

3.1 Experiment

The second experimental site, the Shimohsa Deep Borehole Observatory at Shonan-machi, Chiba Prefecture, is located about 28km away from the Iwatsuki Observatory (Fig. 1). The observation hole is 2.3km in depth (Fig. 2), and the depth of the soil-rock boundary was estimated as 1.5km. The basement rock is Sanbagawa crystalline schist (Suzuki *et al.* 1981).

In the measurement at Iwatsuki, the efficiency of the SH wave generator was confirmed because the generated SH wave was powerful enough to reach at least a depth of 1.5-2.0km. Based on this experience, two S guns of the same capacity, after making a slight reinforcement, were adopted as the source for S wave in this measurement. Simple detonations of dynamite in the shallow shot-hole were supplementarily used too, but only for determining the P wave velocity. By employing two S guns, SH waves having two kinds of onset directions (one, polarized to the south, and the other, polarized inversely to the north) were generated to make an identification of the S wave more reliable. But, one of the S guns unfortunately broke down during the experiment, and the inversely polarized SH wave was observed only for shallower depths of less than 0.5km. Two S guns and four shot-holes were arranged as shown in Fig. 13, and the soil profiles of shot-holes are also shown in the same figure.

The block diagram of the observation system is presented in Fig. 14. The constitution of the system is basically the same as that of the measurement at Iwatsuki. But, in this system, the natural frequency of the borehole receiver is changed to 3.5Hz, and the signals were recorded altogether on a 14 channel data recorder. After the experiment, all the data recorded were digitized at a 0.001sec sampling interval. Based on these digital data, the following data reduction and analysis processes were conducted.

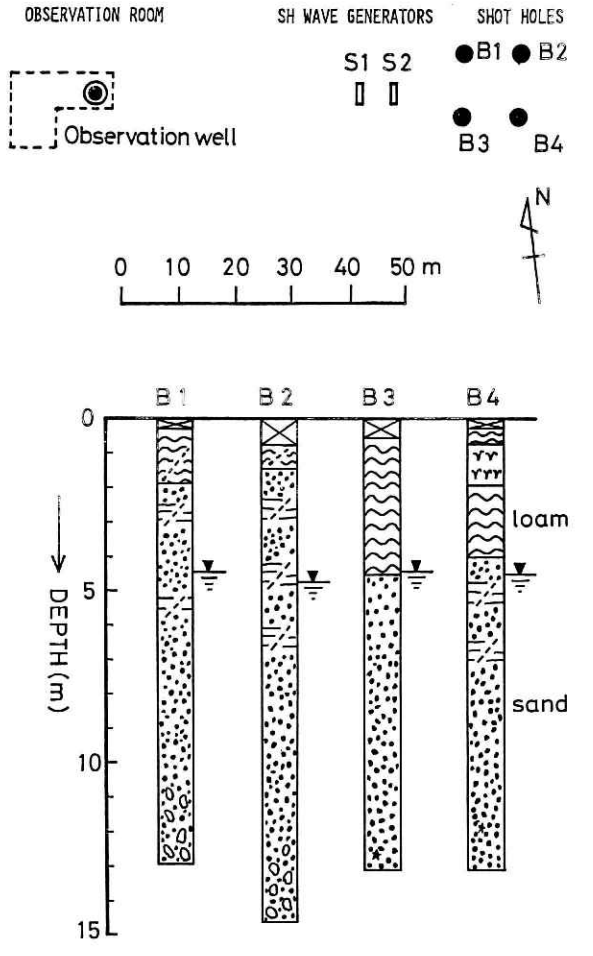

Fig. 13 Plan of the experimental field at Shimohsa. S1 and S2 are two SH wave generators, and B1 through B4 are the shot-holes. Soil profiles of the shot-holes are shown in the lower part.

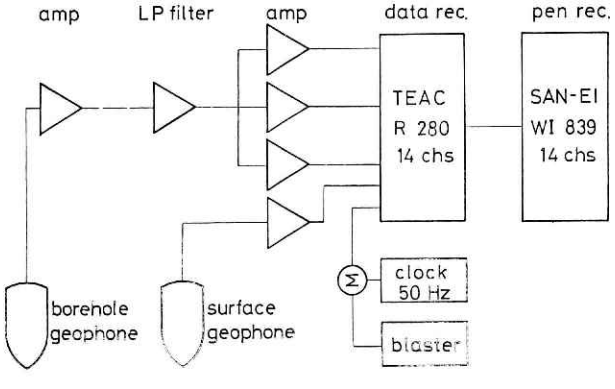

Fig. 14 Block diagram of the observation system for the measurement at Shimohsa.

At the beginning of the experiment, measurement depths had been planned at 17 different depths; however, those were reduced to 15 different depths; that is, at 0.1, 0.2, 0.3, 0.4, 0.5, 0.6, 0.8, 1.0, 1.15, 1.3, 1.45, 1.6, 1.8, 2.05, and 2.3km (the bottom of the hole), because of trouble with the receiver. In spite of the trouble, measurements were completed from the top to the bottom at an interval of 100-250m. The total number of measurements is 73, and the measuring conditions are summarized in Table 3.

3.2 Data and Velocity Structure

Data analysis was done following the method for Iwatsuki, but a digital computer was used for this case. The final SH wave section by the SH wave generator is shown in Fig. 15. In this case, no special effort was made for emphasizing the SH wave as had been done for Iwatsuki. Traces in Fig. 15 were improved only by a simple filtering operation for cutting the frequency higher than 35-40Hz. The identification of the first arriving S waves is immediately done since the onsets are excellently clear on all the traces except for a few traces near 1.3km in depth. The reason why noises preceding the S wave on those records are large for 1.3-1.5km in the depth can be explained by the fact that the cementing of the casing pipe was not completed for those depth ranges (Suzuki 1978, oral communication).

Figure 16 is the paste-up of the P wave section for the vertical component records by means of the simple dynamite explosions in the shot-hole. Though dominant phases corresponding to guided P waves and sound waves in water are similarly recognized, amplitude of the sound wave is markedly smaller than the previous experiment at Iwatsuki.

The relation between travel-time and depth is shown in Fig. 17. The travel-times were similarly corrected for the imaginary source by using the velocity structure in the auxiliary borehole. The velocity profiles of S and P waves deduced from this travel-time curve are compared in Fig. 18 with other known data such as sonic velocities, densities, specific resistivities, and a geological columnar section. The S wave velocity structure is essentially composed of four soil layers and a basement, while for the P wave structure two soil layers lie on the basement. The velocities from the top to the bottom are 0.49, 0.62, 0.82, 1.2, and 2.6km/sec for the S wave, and 2.0, 2.4, and 5.0km/sec for the P wave, respectively. Upper two velocity discontinuities of the S structure in the uppermost soil deposit are not distinguished in the P profile. Since sonic velocities in the depth range from 0.5km to 1.3km gradually increase with depth as shown in Fig. 18, the derived P wave velocity can be interpreted as an average over this depth range. It is also clear that the lower two boundaries of the S and P profiles correspond to those of the geological sec-

Table 3 Specifications of the measuring conditions of the experiment at Shimohsa.

Date Y.M.D.	Meas. Depth (km)	Type	Source Charge (gr)	Depth (m)	Date Y.M.D.	Meas. Depth (km)	Type	Source Charge (gr)	Depth (m)	Date Y.M.D.	Meas. Depth (km)	Type	Source Charge (gr)	Depth (m)
1978	0.1	S2	100		Feb. 16	0.6	S2	150		Feb. 19	1.8	B1	1000	6.5
Feb. 14	0.1	S1	100			0.6	B3	200	12.8		1.8	B3	1000	11.2
	0.1	B1	50	9.7		0.6	B4	100	13.1		1.8	S1	200	
	0.1	B2	50	14.5		0.6	S1	150			1.8	S1	300	
	0.2	S1	200		Feb. 17	0.8	S1	200		Feb. 20	2.3	S1	200	
	0.2	S2	100			0.8	S2	200			2.3	B3	2000	6.1
	0.2	B3	50	13.2		0.8	B1	200	8.6		2.3	B2	3000	13.3
	0.2	B4	100	13.1		0.8	B2	200	14.4		2.3	B4	3100	12.3
						0.8	S2	200			2.3	S1	300	
Feb. 15	0.3	S1	200			0.8	S1	200			2.3	S1	300	
	0.3	S2	100								2.3	S1	300	
	0.3	B1	100	9.7		1.0	S1	300						
	0.3	B3	100	13.2		1.0	B2	300	14.4		2.05	S1	200	
	0.3	S1	200			1.0	B4	300	12.7		2.05	B2	1050	8.0
						1.0	S1	300			2.05	B4	1000	8.1
	0.4	S1	100								2.05	S1	300	
	0.4	S2	100			1.15	S1	300						
	0.4	B1	100	9.7		1.15	B1	300	7.3	Feb. 21	1.6	S1	200	
	0.4	B2	100	14.7		1.15	B3	300	12.5		1.6	B2	500	6.4
	0.4	S1	100			1.15	S1	300			1.6	B4	500	5.5
											1.6	S1	200	
	0.5	S1	150		Feb. 19	1.3	S1	200						
	0.5	S2	150			1.3	B1	300	6.9		1.45	S1	200	
	0.5	B1	200	9.7		1.3	B3	300	12.0		1.45	B2	300	4.1
	0.5	B2	100	14.7		1.3	S1	200			1.45	B4	300	5.5
	0.5	S1	150			1.3	S1	300			1.45	S1	200	
											1.45	S1	200	
Feb. 16	0.6	S1	150			1.8	S1	200			1.45	S1	200	

Type S1 and S2 represent the S-guns, and B1 to B4 are shot-holes.

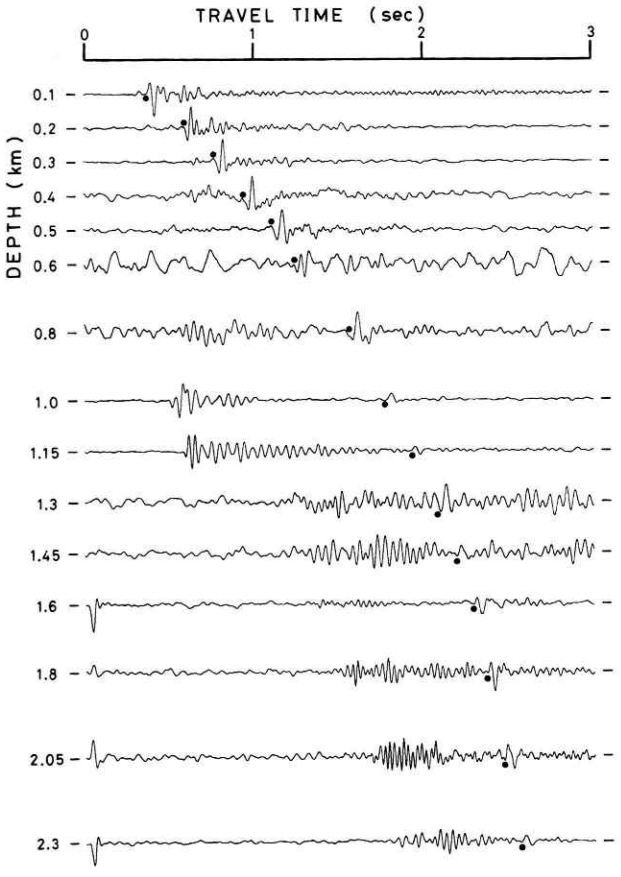

Fig. 15 Paste-up SH waves by the SH wave generator obtained in the measurement at Shimohsa. Solid circles are the onsets of the SH wave.

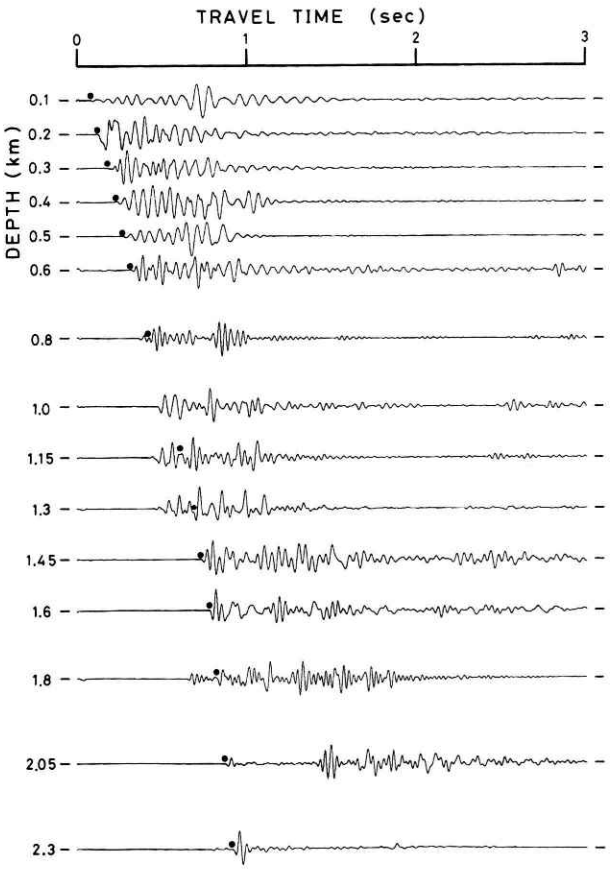

Fig. 16 Paste-up seismograms of the vertical component using small explosions obtained in the measurement at Shimohsa. Solid circles are the onsets of the P wave.

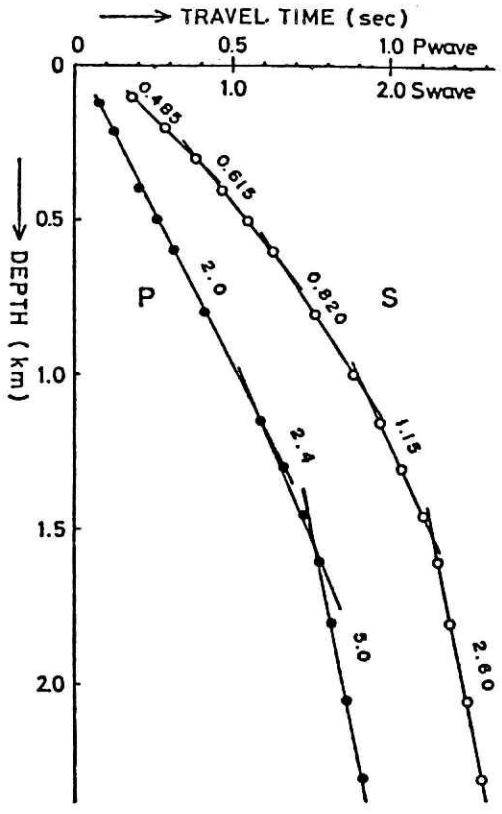

Fig. 17 Travel-time versus depth plots of the S and P waves for the measurement at Shimohsa.

tion, the Pleistocene-Miocene and the Miocene-pre-Tertiary boundaries, respectively. The largest contrast in velocity is seen at the boundary between the soil deposit and basement rock. Gross features of S and P wave profiles are consistent with the logging data as shown in Fig. 18.

4. Design of the New SH wave Generator

On the basis of previous experiments at Iwatsuki and Shimohsa, the validity of the SH wave generator was demonstrated. However, the chamber capacity of the S gun, which is roughly proportional to the power for the SH wave generation, seemed to be insufficient to excite more intensified SH waves that can be clearly observed even at greater depths. Therefore, the new SH wave generator was designed so as to improve mainly the exciting power by enlarging and reinforcing the apparatus (Yamamizu *et al.*, 1981b). The improved points are as follows:

(i) enlarging the powder chamber for generating a more intensified SH wave,

(ii) elongating the gun-barrel for stabilizing the SH wave directivity,

(iii) adopting a symmetrical barrel having muzzles on both ends for exciting right and left polarized SH waves,

(iv) getting better contact with the ground for increasing an efficiency of energy conversion to the SH wave,

and (v) elaborating for easy operation and transportation.

A basic difference between the previous and new S gun is the installation method. The previous type is usually pressed down on the ground by heavy weights, while on the other hand, the new S gun is firmly fixed by driving iron-piles into the ground (Fig. 4). In other words, the new S gun is volumetrically in contact with the ground while the previous one is planely in contact with the ground.

A comparison of SH waveforms originating from the new and previous S guns is shown in Fig. 19. It is clearly seen in this figure that each S gun generates almost the same waveform for various charge sizes, and the SH waves by the new S gun have a rather large amplitude in spite of traveling longer distances than those by the previous type. Accordingly, the new S gun is more efficient for the SH wave generation. The new S gun can be charged up to about 1000gr, so that a more powerful excitation of the SH wave can be obtained.

Figure 20 represents the relation between the charge size and the maximum amplitude of the SH wave generated by the new and old S guns. Assuming that the excitation efficiency is proportional to the gradient of straight lines shown in this figure, the efficiency of the previous S gun is evaluated to be nearly constant to its upper limit of charge size (about 300gr). On the contrary, the efficiency of the new S gun seems to be changed at the 200gr and 400gr charge. That is, the efficiency is slightly higher by about 7% than the previous S gun for the range smaller than 200gr, but surprisingly it becomes almost twice or more for the range of 200-400gr, then falls down to 150% at 400gr.

The abrupt increase of efficiency at the 200gr charge may be caused from the relation between the weight of the S gun itself (about 1 ton) and the kinematic energy of explosion. In the smaller charge range, the S gun is too heavy to be impulsively struck by such a small explosive force. But, even in this range, the new S gun excites stronger SH waves than the previous type because of better volumetrical contact. Above 200gr, the explosive energy becomes sufficient against the weight of the S gun, and it is converted to the SH wave energy with the highest efficiency. The lowering in amplitude at the 400gr charge seems to correspond to a limit of the soil strength. When the slugging force surpasses this limit,

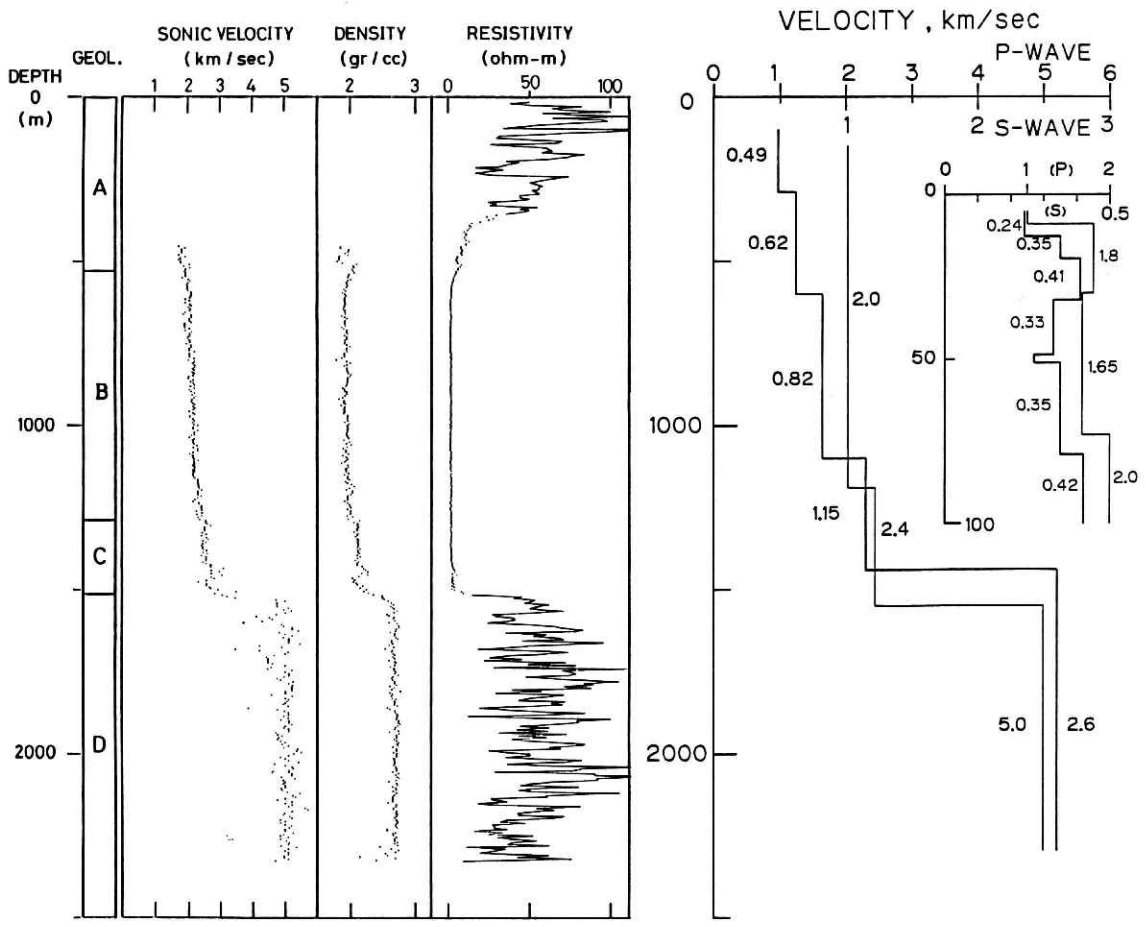

Fig. 18 S and P wave velocity structure at Shimohsa in comparison with the geological section, sonic velocity, bulk density, and electric resistivity. Near surface S and P wave velocities were obtained in a supplementary experiment by means of the conventional technique.

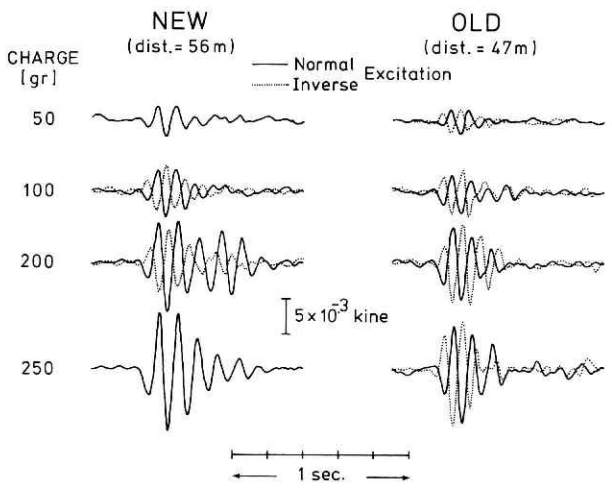

Fig. 19 Comparison of SH waveforms (transverse component of the surface geophone) excited by the old and the new SH wave generator for various charge sizes (weight of black gun powder). Dotted traces are the inverse excitation.

the intimate contact between the soil and iron piles is broken down, and the efficiency is decreased.

It is well known that the excitation efficiency of the S gun is remarkably different under the conditions of installation and composition of the soil (Kobayashi, 1976). Therefore, it is natural that the efficiency may be different in another experimental field under different soil conditions.

5. Measurement at Fuchu

5.1 Experiment

The last experimental site, the Fuchu Deep Borehole Observatory, Fuchu City, Tokyo, is located on the riverbed of the ancient Tama river. This location is about 40km to the southwest of Iwatsuki and 70km to the west-southwest of Shimohsa (Fig. 1). The depth of the observation hole is 2.75km (Fig. 2), and the soil-rock boundary is 2.0km in depth. The basement rock system, which is composed of schale, schalstein, sandstone, tuff, and quarzite, is supposed to belong to the Kobotoke group (Suzuki *et al.*, 1981).

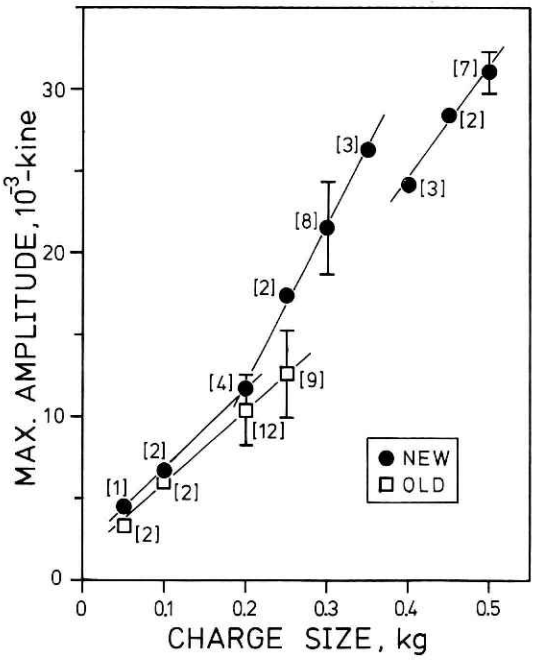

Fig. 20 Relation of the maximum amplitude of the SH wave (transverse component of the surface geophone) by the old and new SH wave generators to the charge size (weight of black gun powder). Amplitude values were averaged over several excitations shown in the brakets.

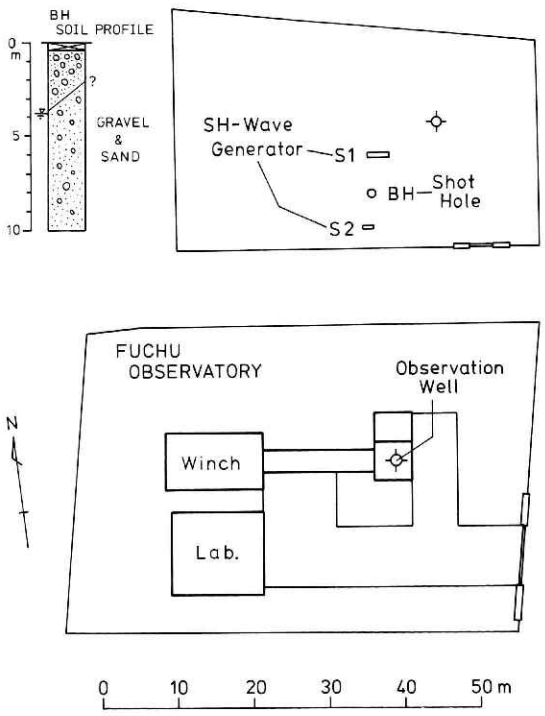

Fig. 21 Plan of the experimental field at Fuchu. S1 is the new SH wave generator, and S2 is the old type one. BH is the shot-hole. Soil profile of the shot hole is shown in the upper-left side.

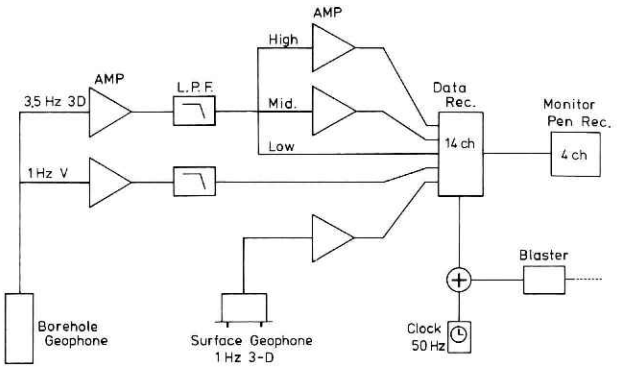

Fig. 22 Block diagram of the observation system for the measurement at Fuchu.

For measurement, the newly designed S gun which was described in the preceding section was used and added to the old-type SH wave generator. Differing from the previous experiments, only one shot-hole was prepared for the P wave source. Two S guns and one shot-hole were arranged on the experimental field as shown in Fig. 21

The observation system, shown in Fig. 22, is essentially the same as the previous measurement systems at Iwatsuki and Shimohsa. The borehole receiver is composed of four seismometers ; that is, one set of the three-component seismometer with a natural frequency of 3.5Hz and one vertical component seismometer of 1Hz. The seismometer of 1Hz was used to examine the decay of surface noises with depth (Yamamizu, 1980). Another set of the three-component seismometer with a natural frequency of 1Hz was operated on the ground surface to check the efficiency of the new S gun in comparison with the previous one.

Measurements were conducted at 17 different depths ; that is, at 0.1, 0.2, 0.3, 0.4, 0.5, 0.65, 0.8, 0.95, 1.1, 1.3, 1.5, 1.75, 2.0, 2.2, 2.4, 2.6, and 2.75km (the bottom of the hole). The total number of blasts were 82. The measuring conditions are summarized in Table 4.

5.2 Data and Velocity Structure

Figure. 23 is the final SH wave section by the SH wave generator. In spite of introducing the new high-powered S gun, the onset of the S wave is rather ambiguous for the area deeper than 1.75km. The poor SH wave arrival seems to be caused by the ground condition on which the S gun was installed. As can be seen from the soil profile of the shot-hole (Fig. 21), the subsurface layer is made up of unconsolidated sand and gravel, so that the contact of the S gun with the ground is rather loose. Accordingly it seems that a lot

Table 4 Specifications of the measuring conditions of the experiment at Fuchu.

Date Y.M.D.	Meas. Depth (km)	Type	Source Charge (gr)	Depth (m)	Date Y.M.D.	Meas. Depth (km)	Type	Source Charge (gr)	Depth (m)
1980	0.1	S1E	50		Feb. 8	1.1	S1E	300	
Feb.5	0.1	S2E	50			1.1	S2E	250	
	0.1	BH	50	10.8		1.1	S2W	250	
	0.1	S1W	50						
	0.1	S2W	50			1.3	S1E	400	
						1.3	S2E	250	
	0.2	S1E	100			1.3	BH	50	10.1
	0.2	S2E	100			1.3	S1E	350	
	0.2	BH	50	10.6		1.3	S2W	250	
	0.2	S1W	100						
	0.2	S2W	100			1.5	S1E	350	
						1.5	S2E	250	
	0.3	S1E	200			1.5	BH	50	10.1
	0.3	S2E	200			1.5	S2W	250	
	0.3	BH	50	10.6		1.5	S1E	300	
	0.3	S1W	200						
	0.3	S2W	200		Feb. 9	1.75	S1E	500	
						1.75	BH	100	9.9
Feb.6	0.4	S1E	300			1.75	S1W	500	
	0.4	S2E	200						
	0.4	BH	50	10.6	Feb.11	2.0	S1E	200	
	0.4	S1W	300			2.0	S1W	400	
	0.4	S2W	200			2.0	BH	100	10.0
						2.0	S1E	450	
	0.5	S1E	300			2.0	BH	100	10.0
	0.5	S2E	200						
	0.5	BH	50	10.6	Feb.12	2.4	S1E	400	
	0.5	S2W	200			2.4	BH	100	9.9
						2.4	S1E	450	
	0.65	S1E	300			2.4	BH	200	9.9
	0.65	S2E	200			2.4	BH	350	9.9
	0.65	BH	50	10.0					
	0.65	S2W	200			2.75	S2E	200	
	0.65	S1E	200			2.75	S1E	500	
	0.65	S2W	200			2.75	S1E	500	
Feb. 7	0.8	S1E	300		Feb.13	2.75	BH	200	10.0
	0.8	S2E	200			2.75	BH	300	9.8
	0.8	BH	50	10.0					
	0.8	S2W	200			2.6	S1E	500	
	0.8	S1E	250			2.6	BH	200	8.3
	0.8	S2W	250			2.6	BH	300	6.0
						2.6	S1E	500	
	0.95	S1E	350						
	0.95	S2E	250			2.2	S1E	500	
	0.95	BH	50	10.2		2.2	BH	200	5.2
	0.95	S2W	250			2.2	BH	100	5.2
	0.95	S1E	250			2.2	S1E	500	
	1.1	S1E	300						
	1.1	BH	50	10.2					

S1, S2, and BH represent two S-guns and shot-hole, E and W added to S1 and S2 represent the excitation direction, East and West.

of explosive energy was absorbed or lost without being converted to the SH wave.

Under such circumstances, the first arrival of the SH wave was identified on horizontal component records which should predominantly catch the SH wave. The horizontal records were processed by operating a filter changing its pass-band systematically or by applying the azimuth converter (Fig. 8) in order to emphasize expected SH waves. The appropriate pass-band was determined by referring to the previous experiments in Iwatsuki and Shimohsa. The previous experiments had revealed that the true SH wave could be distinguished to a certain extent from the ground noise or undesirable phases, for example a P wave in water, by precisely investigating differences of waveforms or interval velocities within them. And in general, the SH waves have a gradually longer period with increasing depth. Referring to those facts, and foreseeing the S wave arrival time based on the velocity structures at Iwatsuki and Shimohsa, the SH wave first arrival was guessed then emphasized by the most preferable filtering operation. Solid circles in Fig. 23 are the onset of the SH wave thus identified.

The P wave section is shown in Fig. 24. Again in this figure, the guided P wave and the sound wave in water are clearly recognized. Amplitudes of the sound wave are apparently very large for the range deeper than 1.5km. Precursory guided waves appear at all depths shallower than 1.3km, while those dominate exclusively at the 2.4km depth for the area deeper than 1.5km. It is uncertain why the guided wave appears in such a manner.

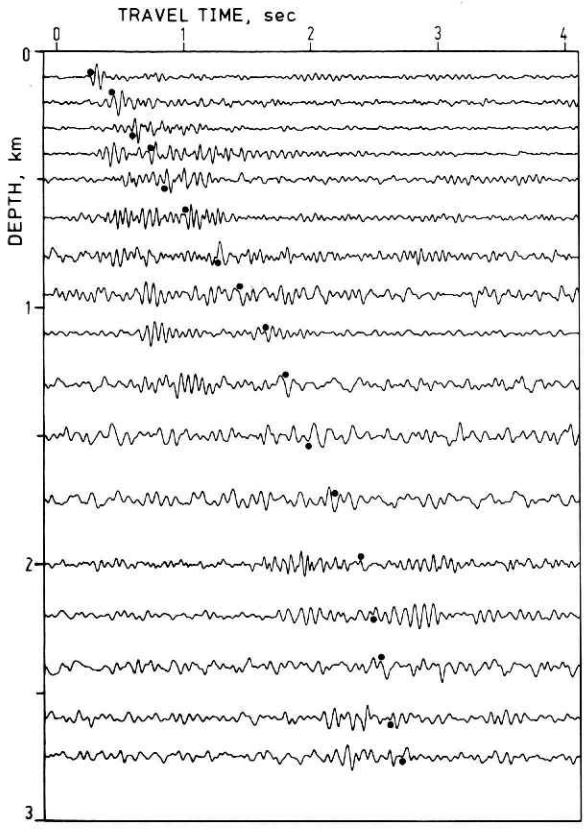

Fig. 23 Paste-up SH waves by the SH wave generator obtained in the measurement at Fuchu. Solid circles are the detected onsets of the S waves.

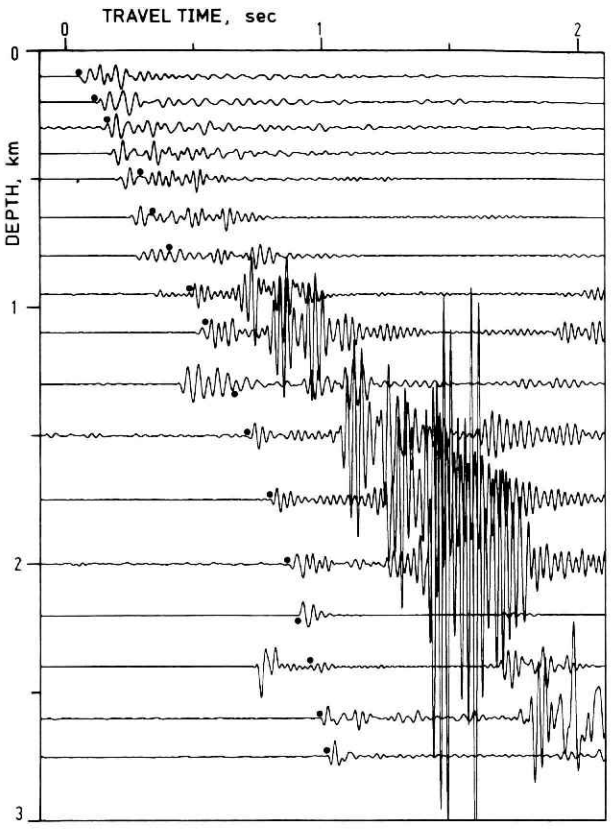

Fig. 24 Paste-up seismograms of the vertical component by small explosions obtained in the measurement at Fuchu. Solid circles are the onsets of the P waves.

Based on these S and P wave sections, arrival times of each phase were read and corrected for the imaginary source, then interval velocities were computed. Figure 25 is the travel-time versus depth relation thus obtained. The velocity profiles of S and P waves are shown in Fig. 26 together with the geological profile and logging data of sonic velocity, density, and resistivity. The most sharp discontinuity in both the S and P wave velocities is clearly recognized at the depth of 2.0km, which completely agrees with the depth of the soil-rock boundary. On the basement rocks, three soil layers are stratified. The velocities of these layers and the basement are 0.54, 0.78, 1.19, and 2.53km/sec for the S wave, and 1.76, 2.14, 3.24, and 4.76km/sec for the P wave, respectively. The depths of the layer boundaries for the S and P profiles are not always consistent with each other. The boundaries in the P profile are slightly deeper than those in the S profile. As shown in Fig. 24, P wave arrivals near those boundaries (0.3-0.5km, and 1.1-1.3km) are strongly contaminated by the precursory guided waves, so that travel-times at those depths seem to be less reliable. Due to this uncertainty, the layer boundaries in the P profile may be movable to a small extent by alternative readings of the P wave arrival time at those depths. The depth discrepancy may also be interpreted as a result of the assumption that the velocities change stepwise with respect to the depth. In spite of the small uncertainties described above, gross features of both S and P wave velocity structures are in good harmony with the logging data and the geological profile.

6. Discussion

6.1 Summary of Velocity Structures

Distributions of the S and P wave velocity in deep soil deposits were revealed by direct and systematic in-situ measurements at three sites, Iwatsuki, Shimohsa, and Fuchu, in the Tokyo metropolitan area. For these sites, the results are in good harmony with the sonic, density, and resistivity logging data, and the geological profile. This demonstrates that the measurements are highly reliable.

The results are summarized in Table 5, and Fig. 27 and 28. In those figures, corresponding boundaries are

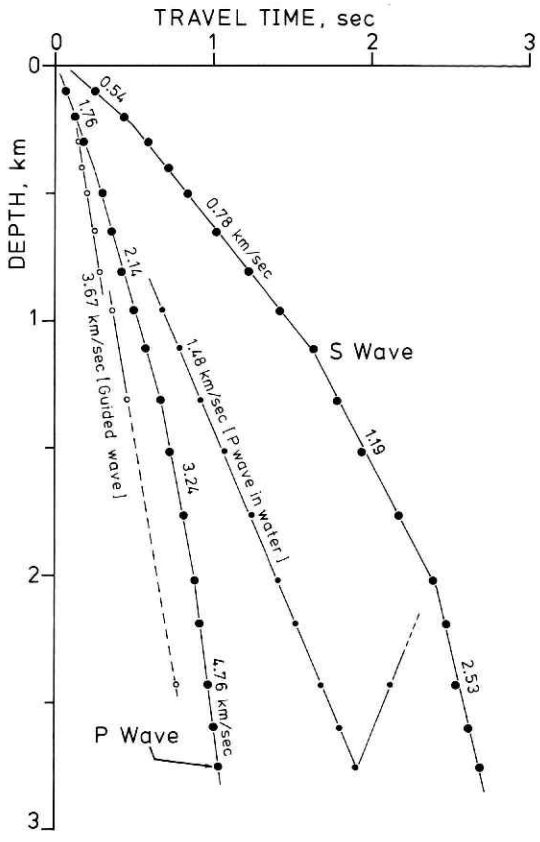

Fig. 25 Travel-time versus depth plots of S, P, and other marked wave groups for the measurement at Fuchu.

indicated by classifying S and P wave velocities into three or four groups as

Fuchu	Iwatsuki	Shimohsa
0.54km/sec ···	0.44km/sec ···	0.49km/sec
? ·····	? ·····	0.62
0.78	0.76	0.82
1.2 ·····	1.3 ·····	1.2
? ·····	1.6 ·····	?
2.5 ·····	2.5 ·····	2.6

for the S wave, and

Fuchu	Iwatsuki	Shimohsa
1.8km/sec ·····	1.8km/sec ·····	2.0km/sec
2.1	2.1	
3.2 ·····	2.9 ·····	2.4
4.8 ·····	4.7 ·····	5.0

for the P wave. Except for one point at Iwatsuki where a layer with an S wave velocity of 1.6km/sec appears, the three sites show an excellent resemblance in their velocity profiles. The somewhat different feature at Iwatsuki is consistent with the geological evidence that the lower Miocene soils are considerably thick at Iwatsuki but very thin or even lacking at both Shimohsa and Fuchu. The S wave velocity structure of Fuchu is very similar to that of Shimohsa, except that the surface of the basement is located 0.5km deeper than that of Shimohsa. A common feature at the three sites is the constant thickness

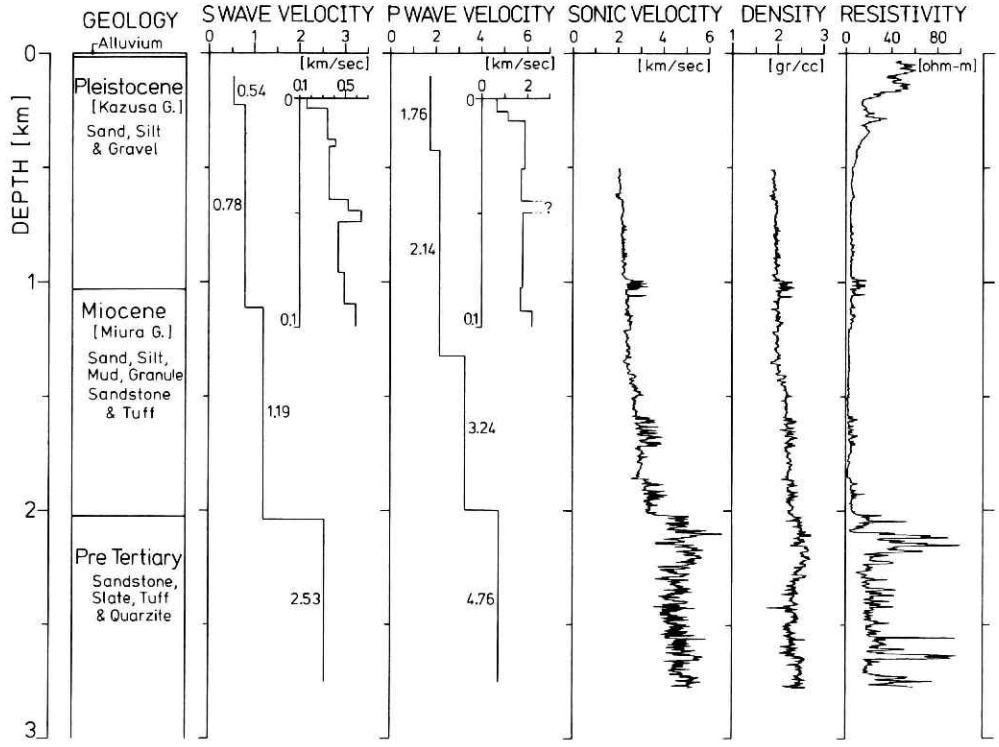

Fig. 26 S and P wave velocity structures at Fuchu in comparison with the geological condition, sonic velocity, bulk density, and electric resistivity. Subsurface (shallower than 100m) structures were obtained in a supplementary experiment by means of the conventional technique.

Table 5 Summary of the S and P wave velocities at Iwatsuki, Shimohsa, and Fuchu.

Iwatsuki				Shimohsa				Fuchu			
Vs (km/s)	Depth (km)	Vp (km/s)	Depth (km)	Vs (km/s)	Depth (km)	Vp (km/s)	Depth (km)	Vs (km/s)	Depth (km)	Vp (km/s)	Depth (km)
0.44		1.80		0.485				0.54		1.76	
	0.32		0.33		0.29				0.23		0.43
				0.615							
					0.60						
0.76		2.10		0.82		2.04		0.78		2.14	
	0.99		1.0		1.10		1.19		1.11		1.32
1.30		2.90		1.15		2.44		1.19		3.24	
	1.97		2.70		1.44		1.55		2.04		2.00
1.60											
	2.80										
2.50		4.70		2.60		4.98		2.53		4.76	

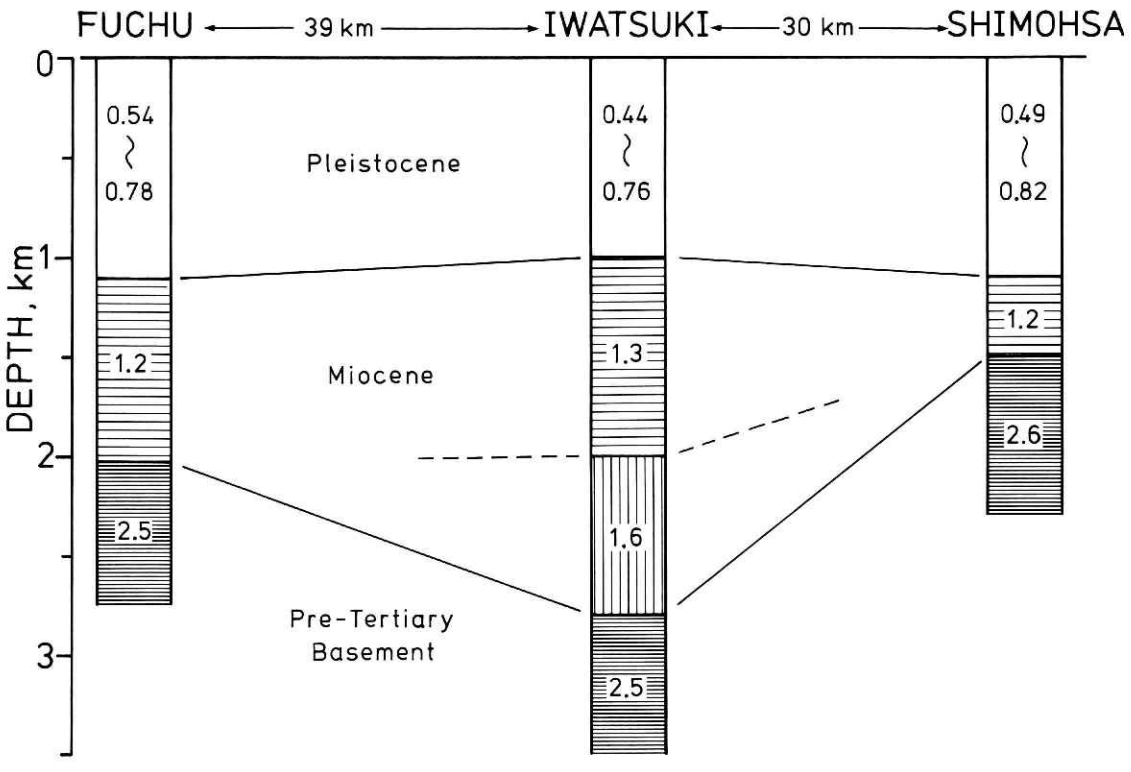

Fig. 27 Comparison of the S wave velocity structure at three deep borehole observatories, Fuchu, Iwatsuki, and Shimohsa.

(about 1.0km) of the uppermost soil layer, notwithstanding differences of the basement depth. Judging from the results by seismic prospecting in the same area (Shima *et al.*, 1976a,b, 1978a,b, 1981), this feature of the uppermost layer seems to continue to the central part of the Tokyo metropolitan area, or at least in the area surrounding the three measurement sites.

The S wave velocities in the soil deposits show rather small changes, and the maximum velocity contrast appears at the soil-rock boundary. This feature of S wave velocities is, in general, also true for P wave velocities (see Fig. 12, 18, and 26). The rate of increase of velocity with depth in the sedimentary layers is much larger in the S wave than in the P wave, which indicates that the wave modification and amplification in the soil deposits is strong for S waves. In addition, the basement material with S wave velocities of 2.5-2.6km/sec and P velocities of 4.7-5.0km/sec is mainly composed of pre-Tertiary or

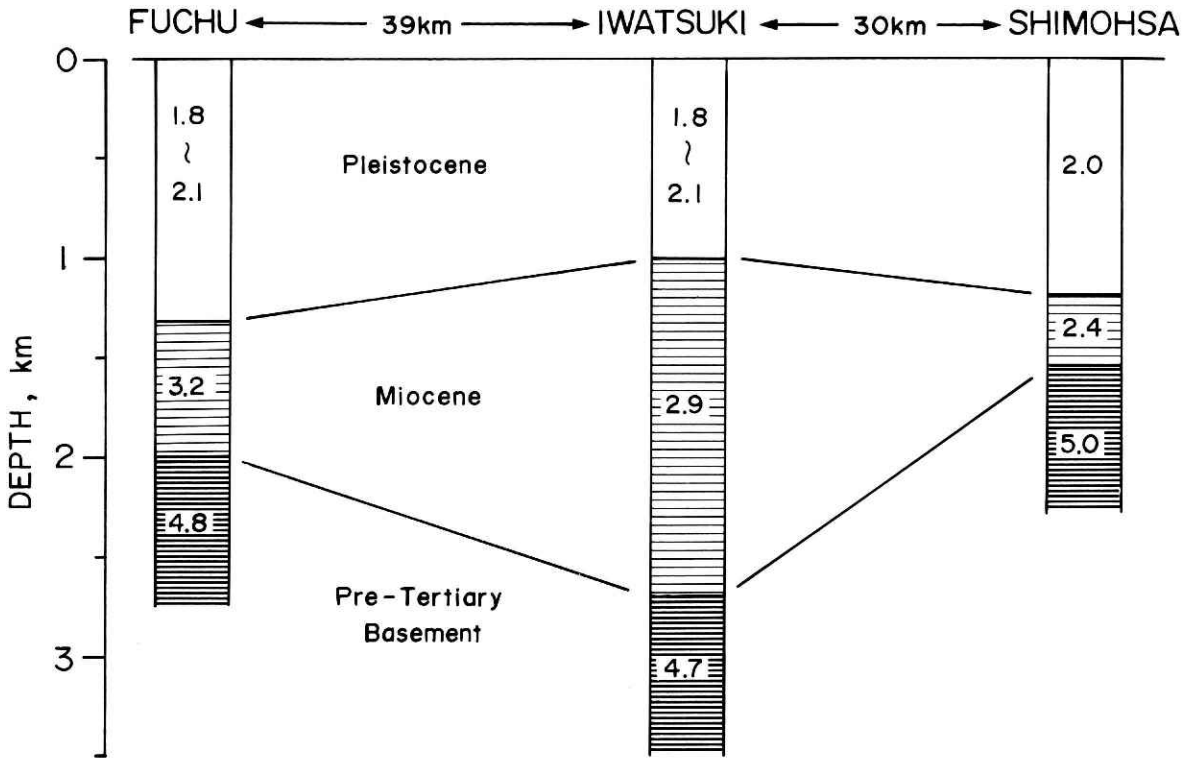

Fig. 28 Compasison of the P wave velocity structure at three deep borehole observatories, Fuchu, Iwatsuki, and Shimohsa.

pre-Neogene metamorphic rocks which are widely spread in and around the Tokyo metropolitan area (Ishii, 1962 ; Fukuda *et al.*, 1974). Therefore, it is reasonable to consider the basement as a so-called "seismic bedrock".

Recently, Shima *et al.* (1976a,b, 1978a,b, 1981) vigorously progressed seismic prospects in order to explore the distribution of the basement beneath the Tokyo metropolitan area by using large-scale explosions at Yumenoshima. Here, we compare the P and S wave velocities of the present results with those past studies. Three prospect lines (see Fig. 30) from Yumenoshima to Yoshikawa (Yu-Ys line), to Takao (Yu-Ta line), and to Tsukuba (Yu-Ts line) are available for comparison with Iwatsuki, Fuchu, and Shimohsa, respectively. Relations are obtained as,

IWT	Yu-Ys line	FCH	Yu-Ta line	SHM	Yu-Ts line
1.8	1.8	1.8	1.5	2.0	1.8
2.1		2.1	2.1		
2.9	2.8	3.2	3.1	2.4	2.6
4.7	5.65	4.8	5.3	5.0	5.6

for the P wave, and

IWT	Yu-Ys line	FCH	Yu-Ta line	SHM	Yu-Ts line
0.44	0.58	0.54	0.63	0.49	
0.76	0.70	0.78		0.62	0.66
				0.82	
1.3	1.5	1.2	—	1.2	1.3
1.6					
2.5	3.0	2.5	—	2.6	2.9

for the S wave, in km/sec unit. For P waves, both measurements are highly consistent with each other. Besides, the consistency of the S wave velocity between them seems good. However, the reliability of the S wave velocities by the refraction studies is not guaranteed because the explosion excites only poor S waves.

6.2 S wave Velocities and Geological Conditions

It is very useful to correlate S wave velocities to geological profiles. If the relation is fully established, the geological structure is immedietly converted into the S wave velocity structure. Ohta and Goto (1976, 1978) tried to find an experimental formula for estimating S wave velocities in terms of characteristic indices of soil including geological conditions. Disappointedly, the formula obtained was applied only to near-surface soils of 0.1-0.2km in depth. It is necessary that the correlation rules be applied to greater depths.

Table 6 represents a relation between seismic wave velocities and geological conditions, which summarize the results obtained in the present measurements. The uppermost Pleistocene layers with an S velocity of 0.4-0.9km/sec and a P velocity of 1.8-2.2km/sec

Table 6 Relation between seismic wave velocities and the geological conditions.

Geological condition		Seismic wave velocity (km/sec)	
Age	Group or Formation	S-wave	P-wave
Late Pleistocene or Pliocene	Narita G. (I,S) Kazusa G. (I,S,F)	0.4-0.9	1.8-2.2
Pliocne or Miocene	Miura G. (S,F) Tokigawa F. (I)	1.1-1.3	2.8-3.2
Miocene	Fukuda F. (I) Arakawa F. (I)	1.6	2.9
pre-Neogene or pre-Tertiary	Basement (I,S,F) rocks	2.5-2.6	4.7-5.0

I, S, and F (Iwatsuki, Shimohsa, and Fuchu, respectively) in parenthesis represent where the geological groups or formations were found.

may be subdivided as follows:

Geology		S wave	P wave
Narita Group		0.4-0.5km/sec	1.8-2.0km/sec
Kazusa Group	Upper	0.5-0.7	
	Lower	0.7-0.9	2.0-2.2

It is clear from Fig. 27 that the S wave velocities in the same geological conditions excellently agree with each other at all the sites. Although the data number is limited, this fact shows that the geological conditions may be effective for estimating the S wave velocities. A similar relation as in Table 6, but for only the P wave velocity, was suggested by Seo *et al.* (1982), in which P velocities locally prospected on outcrop rocks in the Kanto district were used.

In the Kanto Plane, there are more than twenty stratigraphical drillings or pilot-borings for natural gas. The geological profiles in those boreholes were examined in detail, and a comparison among those wells was made by Fukuda *et al.* (1974). The geological structures of those boreholes can be used for extending the 3-D structures of Fig. 27 and 28 into a larger area by using the relation presented in Table 6.

6.3 Velocity in the Basement

A consistency between the present down-hole measurement and the ordinary seismic prospects using Yumenoshima explosions was confirmed as described in Section 6.1. By carefully comparing both results, however, it is found that the velocities in the basement are systematically different in both P and S waves; P and S velocities are 4.7-5.0km/sec and 2.5-2.6km/sec in the present results while they are 5.3-5.7km/sec and 2.9-3.0km/sec, respectively, in the Yumenoshima experiments.

For those velocity differences, two interpretations are possibly related to the method of measurements. The present experiment adopts the down-hole method that directly measures a velocity in the vertical direction while the Yumenoshima experiment is based on the ordinary refraction method in the horizontal direction. The first possibility is an anisotropy of basement rocks. It is well known that the seismic wave velocities in horizontally stratified sedimentary rocks are generally larger in the horizontal direction than in the vertical direction. Since a velocity difference occasionally exceeds over 30% (Postma, 1955; Vander Stoep, 1966; Kitsunezaki, 1971; Bamford and Crampin, 1977; Crampin *et al.*, 1984), the anisotropy may potentially account for the velocity discrepancy. The second possibility is a velocity change within the basement. The present down-hole method measures the so-called interval velocity, so that there is no influence from the velocity distribution outside the concerned interval. In the refraction method, however, apparently a larger velocity may be obtained when the velocity increases with increasing depth beneath the concerned boundary.

Although a definite conclusion cannot be drawn so far, the first possibility of an anisotropy does not seem to be the case. In Table 7, we show the velocities measured in a laboratory for rock-cores which were sampled from the basement when drilling the borehole. Those velocities do not indicate positive evidence for a systematic deviation of sonic wave velocity in any direction. Therefore, it is preferable to adopt the second reason. A recent study by Kasahara

Table 7 Sonic wave velocities of core samples of the basement rock.

Observatory	Sampling depth (km)	Sonic wave velocity (km/sec) Vertical	Horizontal-X	Horizonal-Y
Iwatuski	3.164	4.04	4.08	4.21
	3.324	4.94	4.31	4.37
	3.509	4.52	4.79	—
Shimohsa	1.598	6.70	6.78	5.77
	2.316	4.92	5.12	5.43
Fuchu	2.02	4.01	4.07	4.49
	2.022	4.0	—	3.43
	2.77	3.76	4.03	—

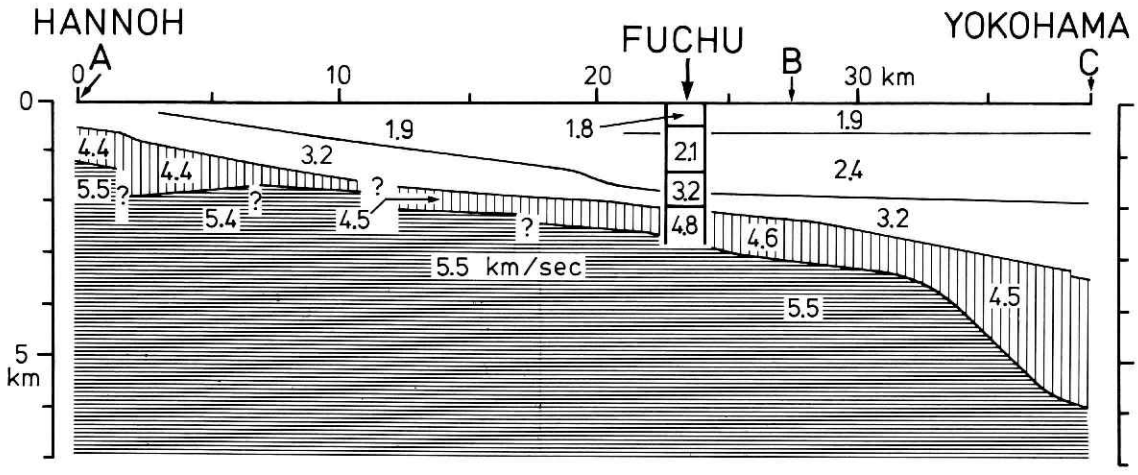

Fig. 29 P wave velocity profile along the line from Hannoh (Saitama) to Yokohama prospected by the refraction method (after Kasahara *et al.*, 1976c). A, B, and C are the shot points. The Fuchu Observatory is located about 2km to the northeast of the section.

et al. (1976c) clearly showed a velocity gradient within the basement. They carried out the precise seismic prospects for determining the depth of the basement before constructing the Fuchu Deep Borehole Observatory. In the experiment, they deployed more than 250 observation points at an interval about 0.15km along a line from Yokohama to Hannoh, and observed signals from three large explosions. In Fig. 29, the P wave structure obtained is shown together with the present result for Fuchu. Though the Fuchu observatory is about 2km apart from the prospect line, both results from vertical and horizontal measurements are excellently consistent. This figure clearly demonstrates the existence of a thin layer with a rather small velocity (Vp=4.4-4.6km/sec) covering the true basement (Vp=5.4-5.6km/sec). Accordingly, the significant difference of the basement velocity may be explained as follows. The present measurements obtained a velocity of the thin layer which constitutes the uppermost part of the basement, while the Yumenoshima experiments measured a velocity of the true basement under the thin layer. In the Yumenoshima experiments, the thin layer might have been masked due to their rather coarse arrangement of observation points.

Recently, Seo and Kobayashi (1980) came to a conclusion of a smaller basement velocity of 5.1km/sec for the P wave along the line from Yumenoshima to Enoshima. This velocity seems to be slightly different from those of the Yumenoshima experiments by Shima *et al.* (1976a,b ; 1978a,b,c). It can be seen in Fig. 29 that the upper layer of the basement becomes two or three times thicker towards Yokohama. Since about half of the observation points of the Enoshima line were located on this area of thick upper-basement, a rather low basement velocity might have been observed. More recently, a low basement velocity was revealed in the same area by another study (Yamanaka, *et al.*, 1986). According to this study, the upper basement with a P velocity of 4.7-4.8km/sec is

widely spread beneath the southwest part of the Tokyo metropolitan area. The thickness of this layer is 2-3km at the maximum. On the other hand, the low velocity basement was not observed in the northern and eastern area of the Tokyo metropolis. However, the present study confirmed the existence of the low velocity basement both at Iwatsuki and at Shimohsa. We, therefore, conclude that the upper layer, despite the fact that it may be very thin, does exist also in the northeastern area of the Tokyo metropolitan area.

6.4 Three Dimensional View of Velocity Structure beneath the Tokyo Metropolitan Area

A three dimensional (3-D) view of the deep underground structure beneath the Tokyo metropolitan area is gradually being brought into light as a result of the accumulation of much data by means of seismic refraction prospects, gravity surveys, stratigraphical drillings, down-hole measurements, and so on (Fig. 30). For example, Shima *et al.* (1978c) summarized the results from refraction prospects in the Tokyo metropolitan area (Higuchi *et al.*, 1977; Kasahara *et al.* 1976a, b, c; and Shima *et al.*, 1976c), and visualized the 3-D undulation of the basement depth in terms of the P wave time-term map. However, the map is mainly focused on the basement, not on the sedimentary layers.

Recently, the author (Yamamizu, 1983) roughly estimated the sediment structures along the prospect lines of Yumenoshima explosions by means of the time-term analysis. In that analysis, the time-term contributions of each sedimentary layer were roughly determined on the basis of the present results of the P wave velocity structure at three sites; Iwatsuki, Shimohsa, and Fuchu (Fig. 28). The thin layer of the uppermost basement (Vp=4.8km/sec) revealed in the previous section was also taken into account. The profiles along Yu-Ys, Yu-Ts, Yu-Do, Yu-Ta, and Yu-En line are shown in Fig. 31 through Fig. 35, respectively. Adding to those profiles, we now construct the geological profile along four lines (broken lines in Fig. 30) by using stratigraphical drillings or

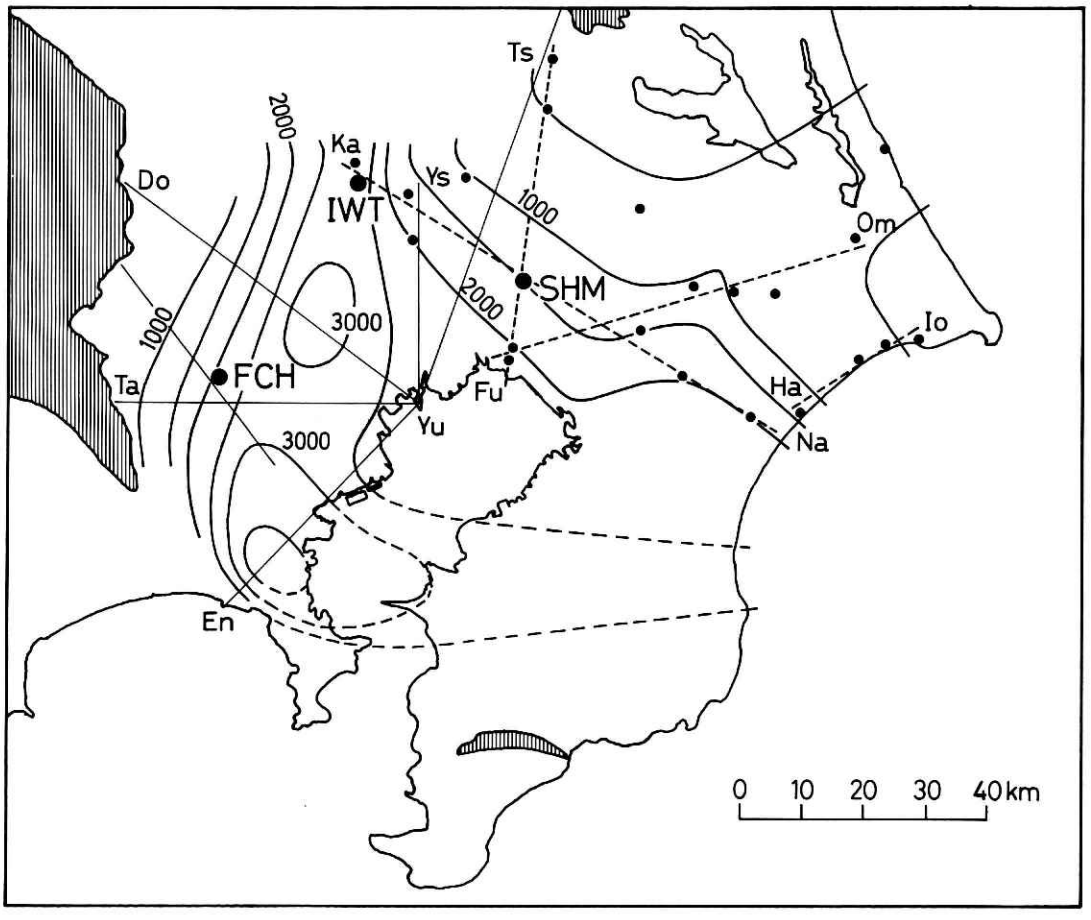

Fig. 30 Distribution of the prospect lines (thin straight lines) and deep boreholes (solid dots). Along the broken lines through dots the geological structure is estimated. The hatched area represents the outcrops of the pre-Neogene basement rocks, and the depth contours of the basement are drawn on the basis of the present results (see Section 6.4).

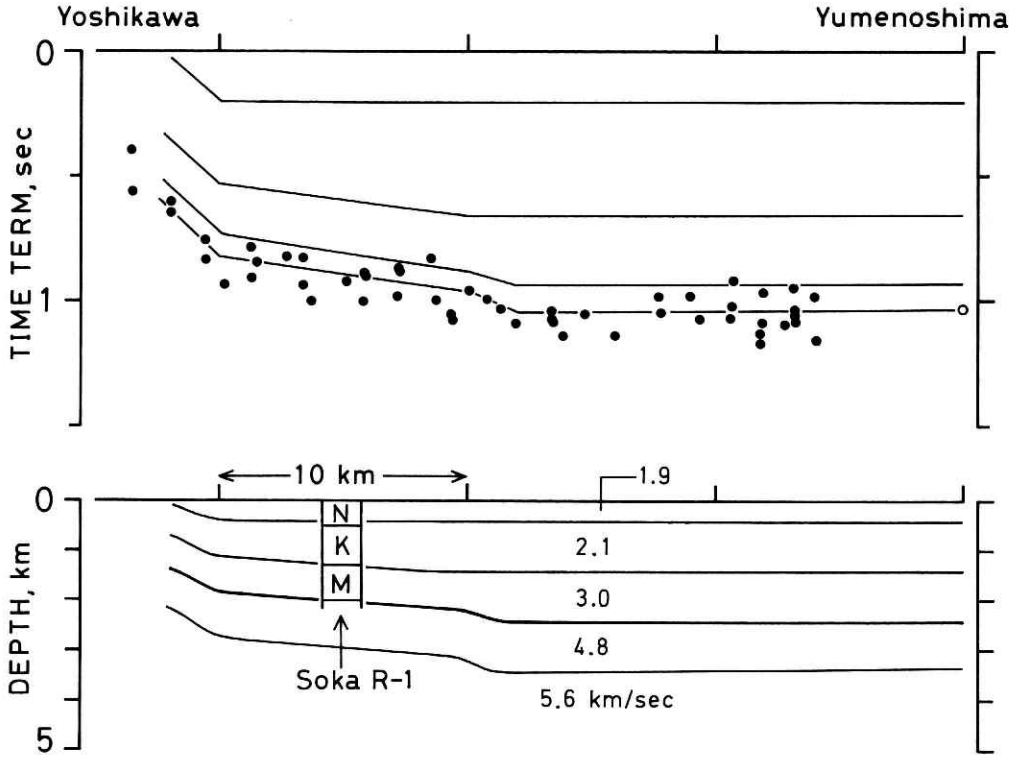

Fig. 31 Subsurface structure (lower) along the line from Yumenoshima to Yoshikawa (Yu-Ys line in Fig. 30). Observed total time-terms and their allotment into the soil layers are shown in the upper figure. For comparison, the geological structure revealed by the stratigraphical drilling of SOKA R-1 is presented.

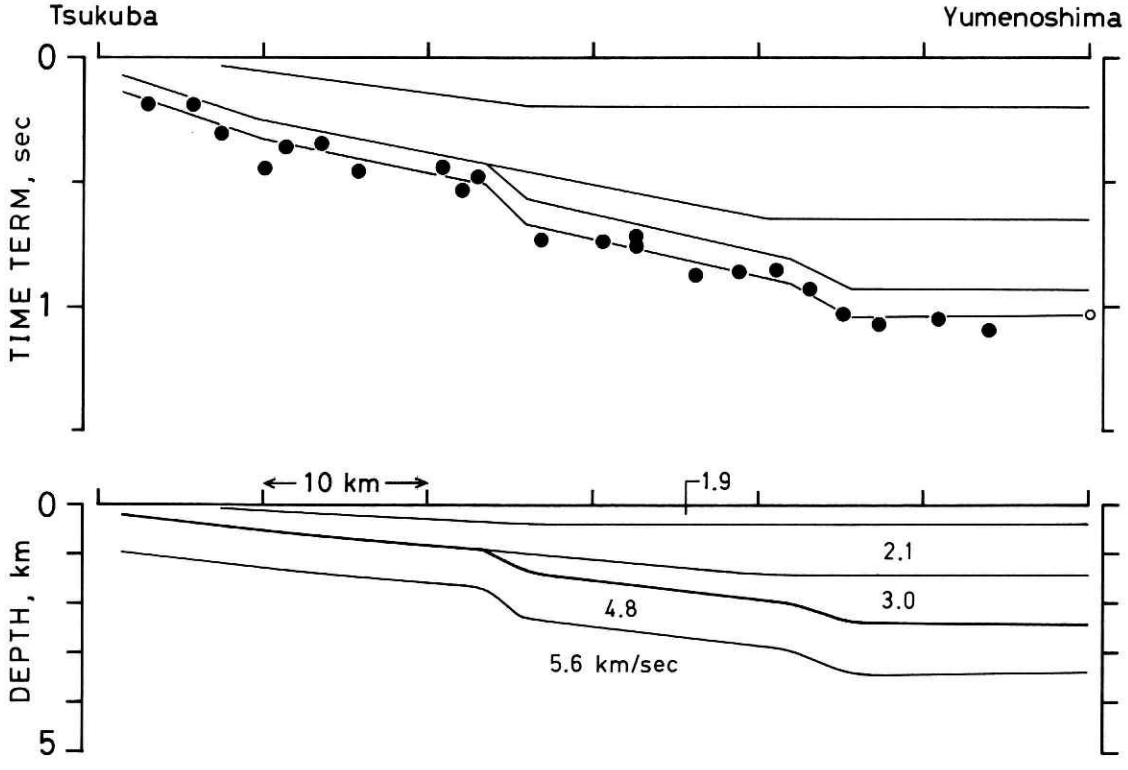

Fig. 32 Subsurface structure (lower) along the line Yu-Ts shown in Fig. 30. Observed total time-terms and their allotment into the soil layers are shown in the upper figure.

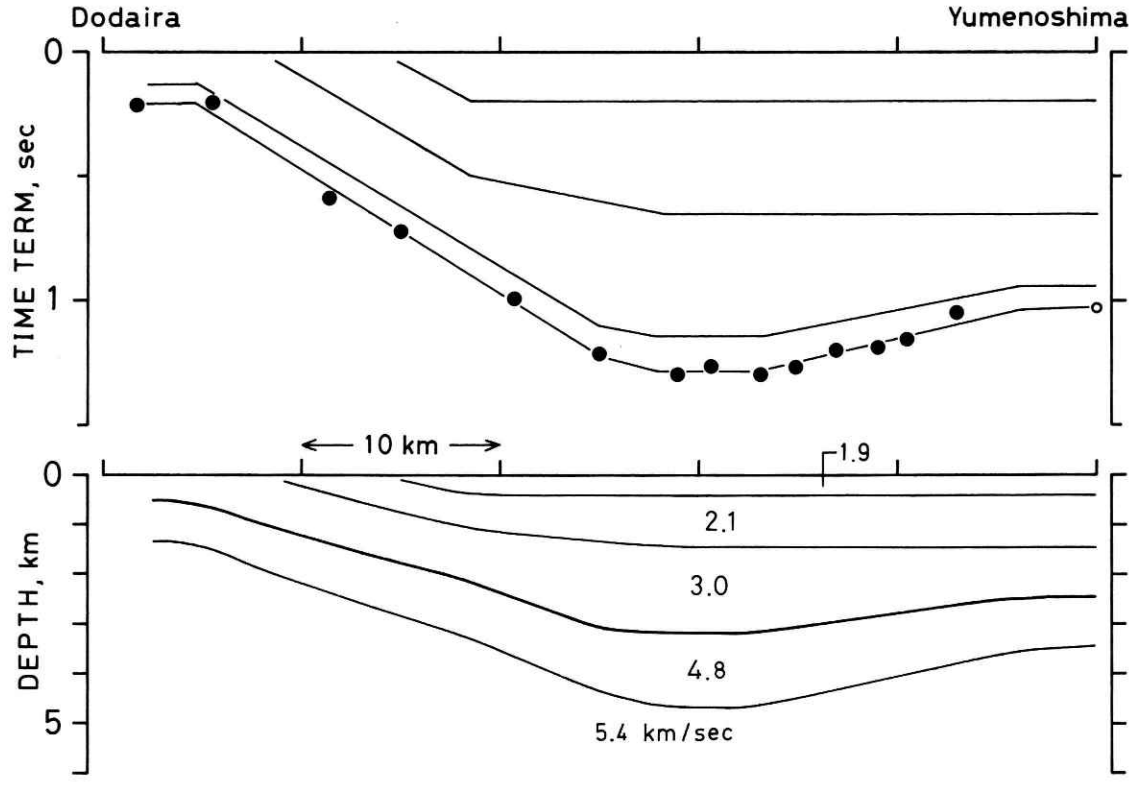

Fig. 33 Subsurface structure (lower) along the line Yu-Do shown in Fig. 30. Observed total time-terms and their allotment into the soil layers are shown in the upper figure.

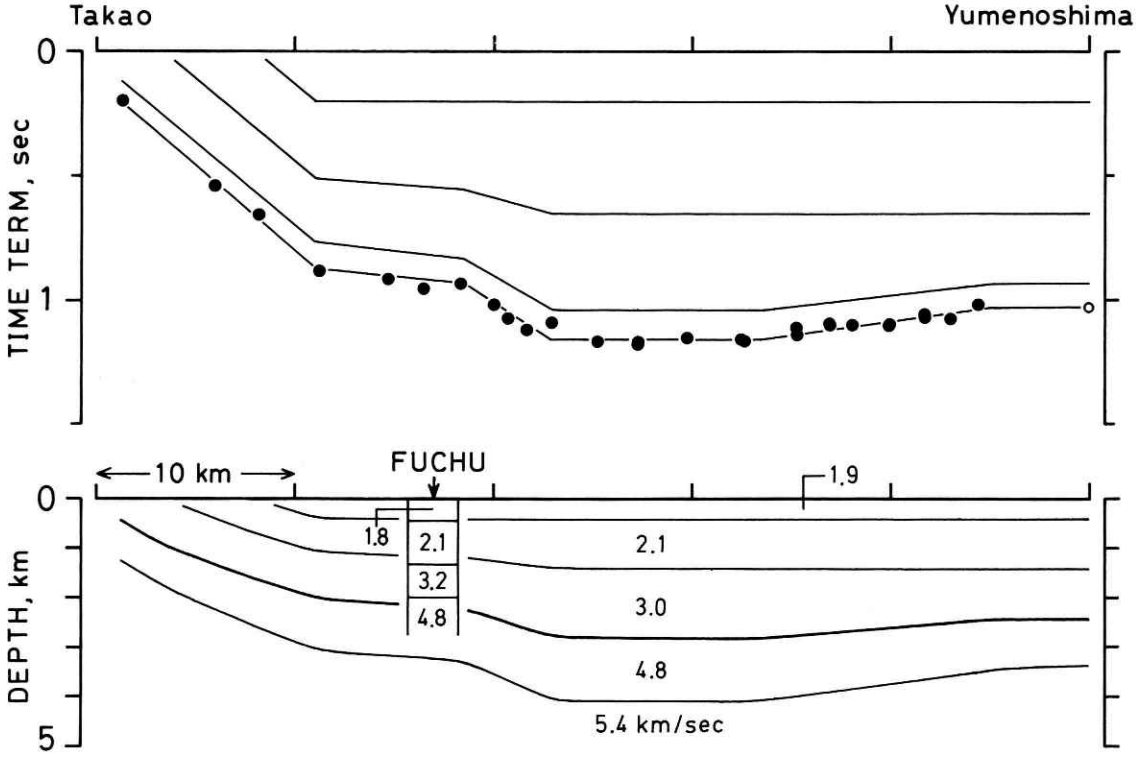

Fig. 34 Subsurface structure (lower) along the line Yu-Ta in Fig. 30 Observed total time-terms and their allotment into the soil layers are shown in the upper figure. For comparison, the velocity structure at Fuchu is presented.

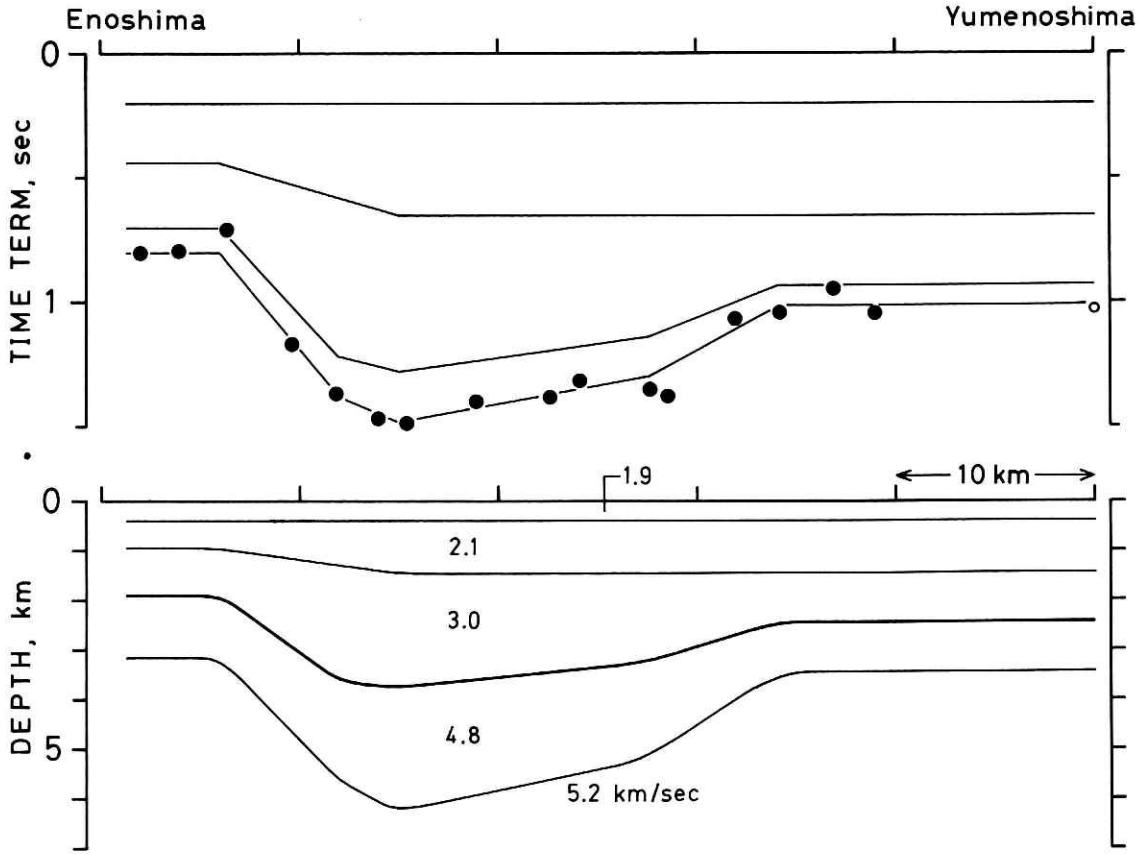

Fig. 35 Subsurface structure (lower) along the line Yu-En in Fig. 30. Observed total time terms and their allotment into the soil layers are shown in the upper figure.

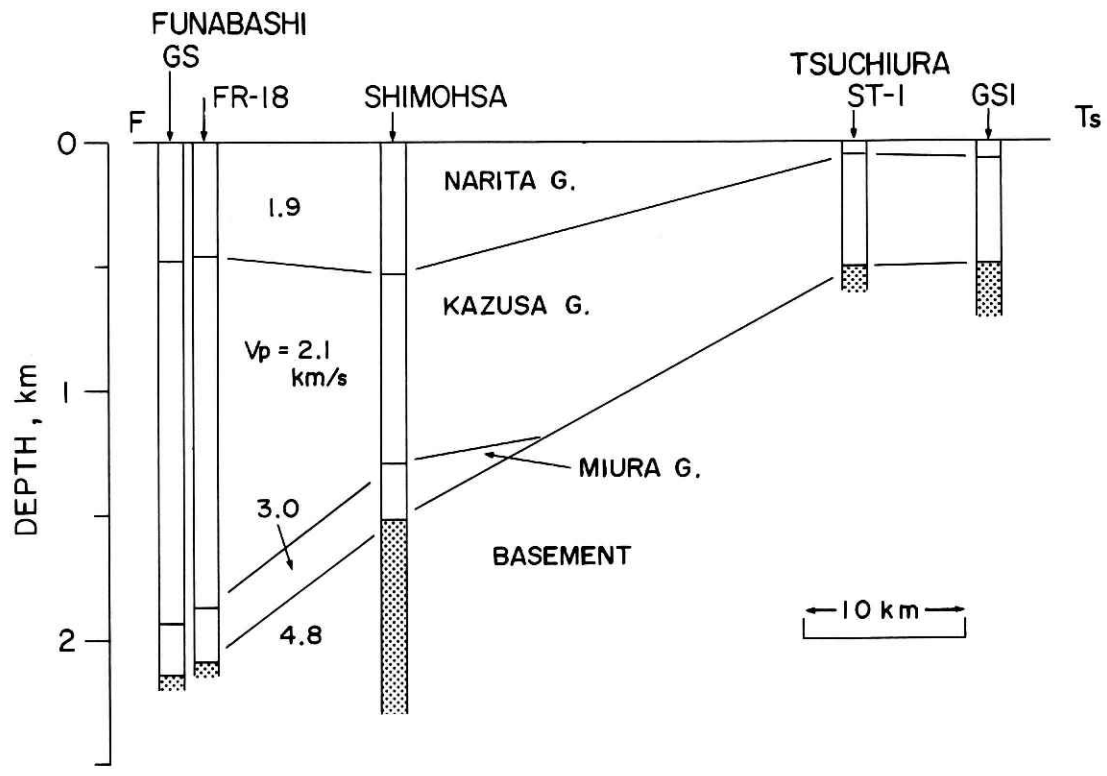

Fig. 36 Geological profile along the line from Funabashi to Tsukuba (broken line Fu-Ts in Fig. 30).

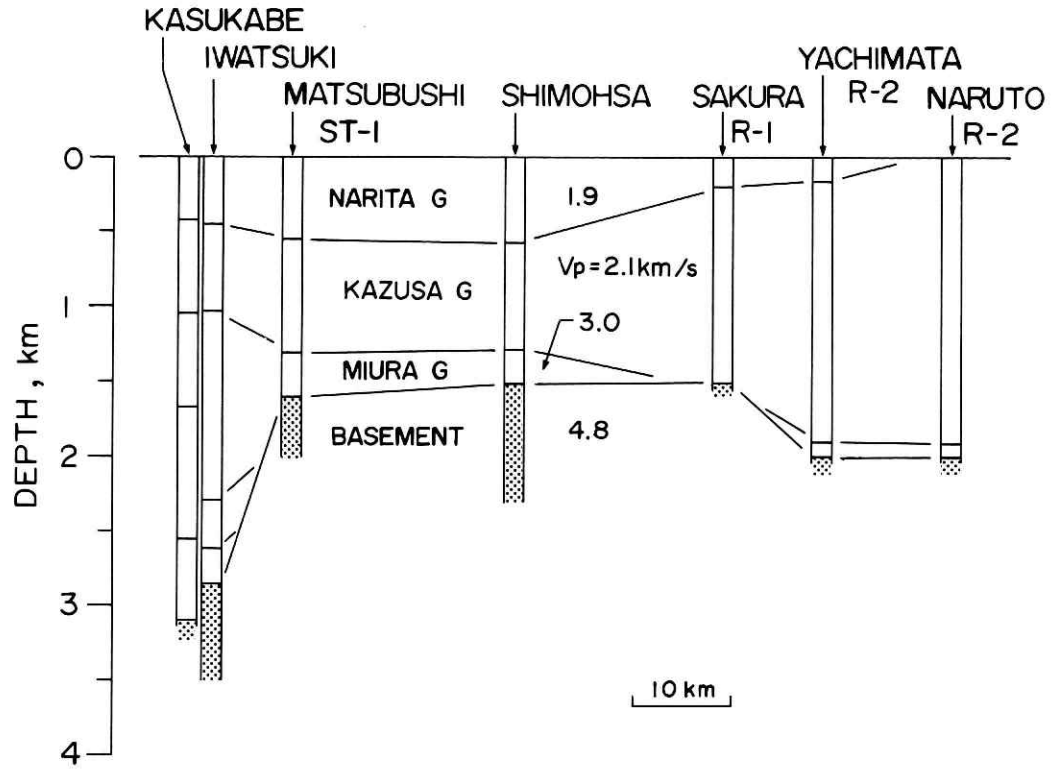

Fig. 37 Geological profile along the northwest-southeast line (broken line Ka-Na in Fig. 30) from Kasukabe to Narutoh.

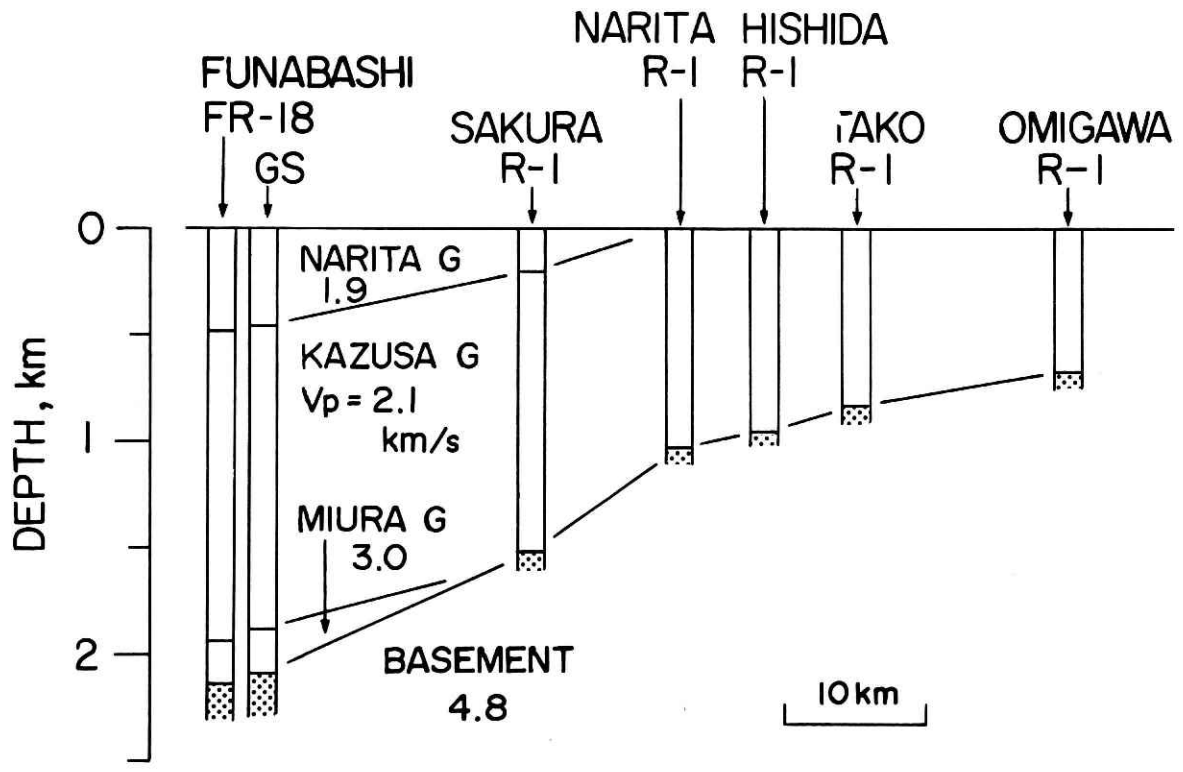

Fig. 38 Geological profile along the line from Funabashi to Omigawa (broken line Fu-Om in Fig. 30).

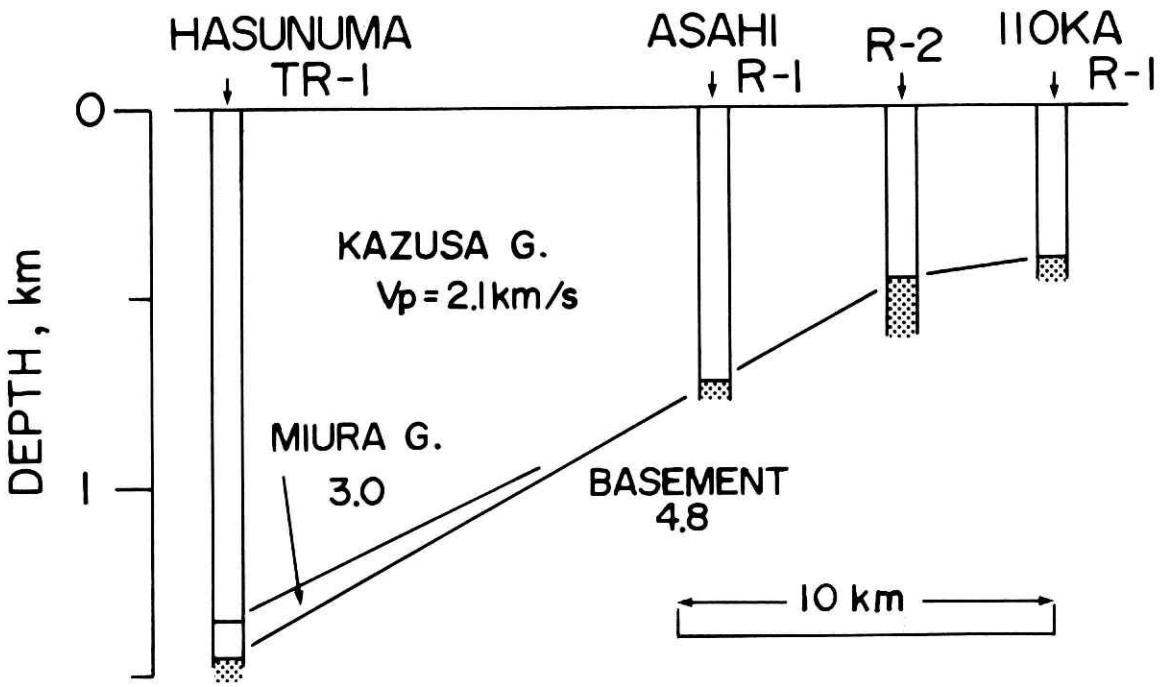

Fig. 39 Geological profile along the line from Hasunuma to Iioka (broken line Ha-Io in Fig. 30).

pilot borings (dots in Fig. 30). The geological profiles from Funabashi to Tsukuba (Fu-Ts), Kasukabe to Naruto (Ka-Na), Funabashi to Omigawa (Fu-Om), and Hasunuma to Iioka (Ha-Io) are shown in Fig. 36 through Fig. 39, respectively. The P wave velocities of each geological formation were assumed as shown in those figures, and were determined on the basis of Table 6 and the subdivision presented in Section 6.2. The velocity of the basement was determined to be 4.8km/sec following the present results.

From those profiles, we are able to reveal the gross feature of the three dimensional distribution of the sedimentary layers and underlying basement in and around Tokyo. However, the 3-D feature of the sediment seems less reliable than the basement. For this reason, we only drew contours of the basement depth as shown in Fig. 30. The 3-D features of the basement are:

(i) the depth is rather shallow (about 1.0-1.5km) in the northeastern area and becomes shallower toward Mt. Tsukuba and Inubo Cape, then the basement crops out at both sites,

(ii) the basement steeply raises up toward the west and ranges to the western mountains,

(iii) the graben-like depression deeper than 3.0km runs from north to south passing through western suburbs of the Tokyo metropolitan area,

and

(iv) the maximum depth of about 3.7km is found in the southern part of Yokohama.

Tada (1982) estimated a similar map of the basement distribution by means of time-term analysis assuming one sedimentary layer over the basement. The 3-D view of the basement shown in Fig. 30 is generally consistent with his results.

It is needless to say that precise prospects, such as Kasahara *et al.* (1976c) shown in Fig. 29, are required in order to widely investigate the 3-D underground structure including the sedimentary layers. This is easy to say, but it is very difficult to do so. This is because human activities are ceaselessly high and enough to disturb the seismic prospects in the Tokyo metropolitan area.

7. Conclusion

The purpose of the present paper is to reveal the seismic wave velocity in deep soil deposits beneath the Tokyo metropolitan area. The distributions of the S wave velocities obtained may be the first direct estimations taken to the depth of 2.3-3.5km in not only Japan but in the world. This knowledge about the S wave will play an important role as fundamental data in the fields of both seismology and earthquake engineering. The conclusions obtained throughout the present paper are summarized as follows:

(1) Profiles of S and P wave velocities to the depth of 2.3-3.5km are obtained by means of the down-hole measurement by using three deep boreholes at Iwatsuki, Shimohsa, and Fuchu in the Tokyo metropolitan area. Those results, summarized in Table 5,

are in good harmony with the sonic, density, resistivity logging data, and the geological profiles of those deep holes (Fig. 12, 18, and 26).

(2) Summarizing the results at the three measurement sites, a simple 3-D view of the underground structure beneath central Tokyo is obtained (Fig. 27 and 28). The structure is generally composed of three layers; the Pleistocene and the Miocene sedimentary layers, and the pre-Tertiary or pre-Neogene basement. The uppermost Pleistocene layer is nearly the same thickness. The basement is the deepest, about 2.8km, at Iwatsuki among the three sites.

(3) A relation between the S and P wave velocities and the geological conditions is obtained (Table 6 and Section 6.2). The velocities of the Pleistocene and Miocene layers are 0.4-0.9km/sec and 1.2-1.9km/sec for the S wave, and 1.8-2.1km/sec and 2.4-3.2km/sec for the P wave, respectively. Those of the basement are 2.5-2.6km/sec and 4.7-5.0km/sec for the S and P waves, respectively.

(4) It was found that the velocity of the basement is systematically different for both the S and P waves between the present measurements and the explorations by the Yumenoshima explosions. The velocity difference strongly suggests that the basement is composed of two layers; a thin layer with a rather small velocity covers the true basement.

(5) The 3-D subsurface structure beneath the eastern part of the Kanto Plain is estimated by using geological data from stratigraphical drillings or pilot borings (Figs. 36, 37, 38, and 39). Together with the results by using Yumenoshima explorations (Fig.31, 32, 33, 34, and 35), the gross feature of the 3-D structure beneath the entire Tokyo metropolitan area is revealed. The depth distribution of the basement with a P wave velocity of 4.8km/sec is presented (Fig. 30).

Since the 17th century, the Tokyo metropolitan area has been the center of political, economic, and cultural activities in Japan, and this area has repeatedly experienced serious damage by large earthquakes such as the Genroku Kanto earthquake in 1703, the Ansei Edo earthquake in 1855, and the Kanto earthquake in 1923 to name a few. Nowadays, human activities are increasing still more and more and they are accompanied with the development of heavy industries, commerce, traffic, and transportation. In this situation, a large earthquake will heavily reduce the national functions to possible ruin. We, therefore, strongly require a total plan to mitigate an earthquake hazard. Finally, the author hopes that the present results will make some contributions to such an earthquake disaster reduction plan.

Acknowledgements

I wish to express my sincere thanks to Prof. Y. Ohta at the Earthquake Research Institute, University of Tokyo, who led me in the S wave velocity measurement by using the deep holes of the National Research Institute for Earth Science and Disaster Prevention (NIED). I also wish to express my thanks to Prof. N. Goto at Muroran Institute of Technology for cooperating with me throughout the present measurements. I would like to thank Prof. M. Ohtake at Tohoku University, Dr. K. Hamada at NIED, and Dr. H. Takahashi at Sato Kogyo Co. for their encouragement and suggestions.

Various information about the geology and the condition of the three deep holes were obtained by Dr. H. Suzuki at NIED. I would like to thank him for his suggestions and warmest support throughout the present work. Also, discussions with the colleagues of NIED were helpful in my progress in this study. I am deeply indebted to all of them.

Thanks must also be extended to the technical crews from Meiho Engineering Co., Akashi Co., Teikoku Oil Co., and Sogo-Chishitu Co. for their cooperation and assistance. Without their assistance, this present study could not have been completed.

Finally, my deepest appreciation is again given to Prof. M. Ohtake at Tohoku University for his critical reading of the manuscript.

References

1) Aki, K. (1982): Strong motion prediction using mathematical modeling techniques, Bull. Seismol. Soc. Am., **72** Special Issue, S29-S41.

2) Archuleta, R. J. and S. M. Day (1977): Near-field particle motion resulting from a propagating stress-relaxation over a fault embedded within a layered medium, Trans. Am. Geophys. Union, **58**, 445,.

3) Bamford, D. and S. Crampin (1977): Seismic anisotropy — the state of the art, Geophys. J. R. astr. Soc., **49**, 1-8.

4) Bouchon, M. (1979): Discrete wavenumber representation of elastic wave fields in three space dimensions, J. Geophys. Res., **84**, 3609-3614.

5) Bouchon, M. and K. Aki (1980): Simulation of long-period, near-field motion for the great California earthquake of 1857, Bull. Seismol. Soc. Am., **70**, 1669-1682.

6) Butler, R. and H. Kanamori (1980) : Long-period ground motion from a great earthquake, Bull. Seismol. Soc. Am., **70**, 943-961.
7) Crampin, S., E. M. Chesnokov, and R. G. Hipkin (1984) : Seismic anisotropy — the state of the art : II, Geophys. J. R. astr. Soc., **76**, 1-16.
8) Erickson, E. L., D. E. Miller, and K. H. Waters (1968) : Shear-wave recording using continuous signal method Part II, Later experimentation, Geophysics, **33**, 240-254.
9) Fukuda, O., H. Takahashi, N. Ohyagi, and H. Suzuki (1974) : "Kohsei chisitsu ni miru Kanto-heiya no kiban", Chishitsu-News edited by Geological Survey of Japan, **234**, 8-17 (in Japanese).
10) Halperin, E. I. and A. V. Frolova (1961) : Three component seismic observation in boreholes II, Bull. Acad. Sci. USSR, Geophys. ser. (English transl.), 519-528.
11) Hamada, K., M. Takahashi, H. Takahashi, and H. Suzuki (1978) : Deep borehole measurements of crustal activities around Tokyo, Proceedings International Workshop on Monitoring Crustal Dynamics in Earthquake Zone, pp 474-500.
12) Heaton, T. H. and D. V. Helmberger (1977) : A study of the strong ground motion of the Borrego Mountain, California, earthquake, Bull. Seismol. Soc. Am., **67**, 315-330.
13) Heaton, T. H. and D. V. Helmberger (1978) : Predictability of strong ground motion in the Imperial Valley : modeling the M4.9 November 4, 1976 Brawley earthquake, Bull. Seismol. Soc. Am., **68**, 31-48.
14) Helmberger, D. V. and L. R. Johnson (1977) : Source parameters of moderate size earthquakes and the importance of receiver crustal structure in interpreting observations of local earthquakes, Bull. Seismol. Soc. Am., **67**, 301-313.
15) Higuchi, S., K. Kasahara, K. Ito, T. Yada, A. Ishii, T. Aakagiri, Y. Hara, K. Furuno, H. Suzuki, H. Tsukahara, S. Matsumura, E. Yamamoto, and H. Morei (1977) : Observation of explosional seismic waves in Katsunan region, Chiba pref., Japan, Bull. Chiba Pref. Res. Inst. Environ. Pollut., **7**, 59-64 (in Japanese).
16) Ishii, M. (1962) : Basement of the Kwanto plain, J. Japanese Assoc. Petro. Tech., **27**, 405-430 (in Japanese).
17) Jolly, R. (1956) : Investigation of shear waves, Geophysics, **21**, 904-938.
18) Kakimi, T., Y. Kinugasa, and M. Kimura (compiled) (1973) : Neotectonic Map Tokyo, Tectonic maps ser.2, Geol. Surv. Japan.
19) Kanamori, H. (1974) : Long-period ground motion in the epicentral area of major earthquakes, Tectonophys., **21**, 341-356.
20) Kasahara, K., H. Suzuki, T. Kumagai, I. Hasegawa, and T. Tada (1976a) : "Sayama-kyuryo fukin no souji ijyo ni tsuite", Presented at the annual meeting of Seismological Society of Japan, 53 (1) (in Japanese).
21) Kasahara, K., H. Suzuki, and H. Takahashi (1976b) : "Tokyo-seibu chiku kiban chosa ni tsuite 1", Presented at the annual meeting of Seismological Society of Japan, 54 (1) (in Japanese).
22) Kasahara, K., H. Suzuki, and H. Takahashi (1976c) : "Tokyo-seibu chiku kiban chosa ni tsuite 2" Presented at the annual meeting of Seismological Society of Japan, 139 (2) (in Japanese).
23) Kitsunezaki, C. (1967) : Observation of S wave by the special borehole geophone, Butsuri-Tanko (Geophys. Explor.), **20**, 1-15 (in Japanese).
24) Kitsunezaki, C. (1971) : Field experimental study of shear waves and related problems in soil, Geophys. Inst., Kyoto Univ., Japan, **11**, 103-177.
25) Kitsunezaki, C. (1976) : S wave velocity loggings, Spec. Issue Seismic Explor. Group Japan, 50-56 (in Japanese).
26) Kitsunezaki, C. (1980) : A new method for shear-wave logging, Geophysics, **45**, 1489-1506.
27) Kobayashi, N. (1976) : "S-ha sokutei no imi", in Experimental Studies on Generation and Propagation of Seismic Waves, pp48-50, The Seismic Exploration Group of Japan, (in Japanese).
28) Kovalev, O. I. and L. V. Molotova (1960) : Borehole percussion device for the excitation of various types of elastic waves, Bull. Acad. Sci. USSR, Geophys. ser. (English transl.), 959-969.
29) Kubotera, A. and Y. Ohta (1967) : On seismic waves generated by small explosions, Spec. Contr. Geophys. Inst. Kyoto Univ., **7**, 169-179.
30) Lash, C. C. (1980) : Shear waves, multiple reflections, and converted waves formed by a deep vertical wave test (vertical seismic profiling), Geophysics, **45**, 1373-1411.
31) Macdonal, F. J., F. A. Aagona, R. L. Mills, R. L. Sengbush, R. G. Van Nostrand, and J. E. White (1958) : Attenuation of shear and compressional waves in Pierre Shale, Geophysics, **23**, 421-439.
32) Murphy, V. J. (1978) : Geophysical engineering investigative techniques for site characterization, Proc. 2nd Inter. Conf. Microzonation, San Francisco, USA, 153-178.
33) Ohta, Y. (1968) : Experimental study on generation and propagation of S waves III, Bull. Earthq. Res. Inst., Univ. Tokyo, **45**, 727-738.
34) Ohta, Y. and N. Goto (1976) : Estimation of S-wave velocity in terms of characteristic indicesof soil, But-

suri-Tanko (Geophys. Explor.), **29**, 85-95 (in Japanese).

35) Ohta, Y. and N. Goto (1978): Physical background of the statistically obtained S wave velocity equation in terms of soil indexes, Butsuri - Tanko (Geophys. Explor.), **31**, 96-105 (in Japanese).

36) Ohta, Y., N. Goto, K. Shiono, H. Takahashi, F. Yamamizu, and S. Kurihara (1977): Shear wave velocities in deep soil deposits — Measurement in a borehole to the depth of 3500 meters and its significance, Zishin (J. Seismol. Soc. Japan), Ser.2, **30**, 415-438 (in Japanese).

37) Ohta, Y., N. Goto, K. Shiono, H. Takahashi, F. Yamamizu, and S. Kurihara (1978): Shear wave velocities in deep soil deposits. Part II Measurement in a borehole of Shimofusa observatory to the depth of 2300 meters, Zishin (J. Seismol. Soc. Japan), Ser.2, **31**, 299-308 (in Japanese).

38) Ohta, Y., N. Goto, F. Yamamizu, and H. Takahashi (1980): S wave velocity measurements in deep soil deposit and bedrock by means of an elaborated down-hole method, Bull. Seismol. Soc. Am., **70**, 363-377.

39) Postma, G. W. (1955): Wave propagation in a stratified medium, Geophysics, **20**, 780-806.

40) Seo, K. and H. Kobayashi (1980): On the seismic prospectings in the southwestern part of the Tokyo Metropolitan Area — Underground structure along the line stations from Yumenoshima, Tokyo to Enoshima, Kanagawa-, Zishin (J. Seismol. Soc. Japan), Ser.2, **33**, 23-36 (in Japanese).

41) Seo, K., S. Midorikawa, Y. Mitani, and S. Shu Geun (1982): Deep subsurface ground structure of the southwestern Kanto district, Proceedings of the 6 th Japan Earthquake Engineering Symposium, pp 49-56.

42) Shima, E. and Y. Ohta (1968): Experimental study on generation and propagation of S waves: I. Designing SH-wave generator and its field tests, Bull. Earthq. Res. Inst., Univ. Tokyo, **45**, 19-31.

43) Shima, E., M. Yanagisawa, K. Kudo, T. Yoshii, Y. Ichinose, K. Seo, K. Yamazaki, N. Ohbo, Y. Yamamoto, Y. Oguchi, and M. Nagano (1976a): On the base rock of Tokyo. Observations of seismic waves generarated from the 1 st and 2nd Yumenoshima explosions, Bull. Earthq. Res. Inst., Univ. Tokyo, **51**, 1-11 (in Japanese).

44) Shima, E., M. Yanagisawa, K. Kudo, K. Seo, and K. Yamazaki (1976b): On the base rock of Tokyo. II: Observations of seismic waves generated from the 3rd Yumenoshima and Yoshikawa explosions, Bull. Earthq. Res. Inst., Univ. Tokyo, **51**, 45-61 (in Japanese).

45) Shima, E., M. Yamagisawa, S. Zama, and K. Seo (1976c): Tokyo nanbu no kiban, Presented at the annual meeting of Seismological Society of Japan, 322 (2) (in Japanese)

46) Shima, E., M. Yanagisawa, K. Kudo, T. Yoshii, K. Seo, and K. Kuroha (1978a): On the base rock of Tokyo III. Observations of seismic waves generated from the 4th and 5th Yumenoshima explosions, Bull. Earthq. Res. Inst., Univ. Tokyo, **53**, 305-318 (in Japanese).

47) Shima, E., M. Yanagisawa, K. Kudo, T. Yoshii, K. Seo, N. Ohbo, T. Hoshino, and M. Nagano (1978b): On the base rock of Tokyo IV. Observations of seismic waves generated from the 6th and 7th Yumenoshima explosions, Bull. Earthq. Res. Inst., Univ. Tokyo, **53**, 1245-1255 (in Japanese).

48) Shima, E., M. Yanagisawa, and S. Zama (1978c): On the deep underground structure of Tokyo Metropolitan Area, Proceedings of the 5th Japan Earthquake Engineering Symposium, pp 321-328 (in Japanese).

49) Shima, E., M. Yanagisawa, K. Kudo, and K. Seo (1981): On the base rock of Tokyo V. Observations of seismic waves generated from the 7th, 8th, and 9th Yumenoshima explosions, Bull. Earthq. Res. Inst., Univ. Tokyo, **56**, 265-276 (in Japanese).

50) Stewart, R. R., R. M. Turpening, and N. Toksoz (1981): Study of a subsurface fracture zone by vertical seismic profiling, Geophys. Res. Let., 8, 1132-1135.

51) Suzuki, H., R. Ikeda, T. Mikoshiba, S. Kinoshita, H. Sato, and H. Takahashi (1981): Deep well logs in the Kanto-Tokai area, Rev. Res. Disaster Prevention, 65, pp162 (in Japanese).

52) Tada, T. (1982): Structure of the basement and gravity anomaly in the Kanto plain (1) — Depth distribution of the basement —, Zishin (J. Seismol. Soc. Japan), Ser.2, **35**, 607-618 (in Japanese).

53) Takahashi, H. and K. Hamada (1975): Deep borehole observation of the earth's crust activities around Tokyo — Introduction of the Iwatsuki observatory —, Pure and Appl. Geophys., **113**, 311-320.

54) Takahashi, H. (1982): The deep-borehole observatories and their contribution for revealing the characteristics of microearthquake activity in the Kanto district, Rep. Nat. Res. Centr. Disaster Prevention, **28**, 1-104 (in Japanese).

55) Vander Stoep, D. M. (1966): Velocity anisotropy measurements in wells, Geophysics, **31**, 900-916.

56) White, J. E. and R. L. Sengbush (1963): Shear waves from explosive sources, Geophysics, **28**, 1001-1019.

57) White, J. E. (1965): Seismic Waves, Radiation, Transmission, and Attenuation, MacGraw-Hill, New York.

58) Yamamizu, F., H. Tsukahara, H. Sato, M. Ishida, and K. Hamada (1977): Kawasaki borehole station for microearthquake observation and its vertical distribu-

tion of background noises, Rep. Nat. Res. Centr. Disaster Prevention, **18**, 17-33 (in Japanese).

59) Yamamizu, F. (1980): Depth distribution of ground noise in the Fuchu deep borehole observatory, Presented at the annual meeting of Seismological Society of Japan, B43 (2) (in Japanese).

60) Yamamizu, F., H. Takahashi, N. Goto, and Y. Ohta (1981a): Shear wave velocities in deep soil deposits. Part III — Measurements in the borehole of the Fuchu observatory to the depth of 2750m and a summary of the results —, Zishin (J. Seismol. Soc. Japan), Ser.2, **34**, 465-479 (in Japanese).

61) Yamamizu, F., H. Takahashi, Y. Ohta, N. Goto, and T. Takeyama (1981b): Design of the new SH wave generator, Zishin (J. Seismol. Soc. Japan), Ser.2, **34**, 589-591 (in Japanese).

62) Yamamizu, F. (1983): Structure of sedimentary layers beneath the Tokyo Metropolitan Area, Presented at the annual meeting of Seismological Society of Japan, B58 (1) (in Japanese).

63) Yamamoto, E., K. Hamada, and K. Kasahara (1975): Background seismic-wave noise and elimination of noise transmitted through water in a borehole at the Iwatsuki observatory, Zishin (J. Seismol. Soc. Japan), Ser.2, **28**, 171-180 (in Japanese).

64) Yamanaka, H., K. Seo, T. Samano, and S. Midorikawa (1986): On the seismic prospectings in the southwestern part of the Tokyo Metropolitan Area (2) — Underground structure along the lines from Kurokawa, Kawasaki to Okazu, Yokohama and from Yumenoshima, Tokyo to Nagatsuta, Yokohama —, Zishin (J. Seismol. Soc. Japan), Ser.2, **39**, 607-620 (in Japanese).

(Accepted: 25 August, 1995)

首都圏におけるやや深い構造の地震波速度

山水史生*

防災科学技術研究所

要　旨

首都圏は2～3 kmの厚い堆積層に覆われている．この厚い堆積層の地震波速度構造を詳細に解明することは，地震学及び地震工学的見地から極めて重要である．本論では，首都圏の地震観測を目的に建設された防災科学技術研究所の岩槻・下総・府中深層観測井を利用して，深さ2～3 kmまでの地震波速度構造の直接測定を組織的に行った．地震工学及び耐震工学上はS波速度がP波速度よりも重要なため，測定はS波速度構造に重点を置いたものとし，地表に震源を置き，それからの地震波を観測井内に設置した3成分地震計により記録するDown-hole法により行った．S波震源としては2種類使用した．1つは，少量のダイナマイトの爆発によるものであり，もう1つは，いわゆるS大砲と呼ばれているものである．P波震源はダイナマイト爆発のみである．それぞれの観測井において，地層の変化の激しい浅部では約100 mと間隔を小さくし，安定した深部では250～300 mとやや大きい間隔で，15～17深度で測定を行った．

測定結果は，観測井掘削時に得られている各種検層結果と極めてよく調和しており，精度の高いものであることを示している．3地点での結果を総合してみると，地下構造は基本的に同じ構成であり，堆積層2層が基盤の上に載っているものであることが解明された．各層のS波速度は，上から最新世層が0.4～0.9 km/sec，中新世層が1.2～1.9 km/sec，先新第三紀系または先第三紀の基盤が2.5～2.6 km/secであり，3地点ともほぼ同じ値を示す．同様に，P波速度については，上から1.8～2.1 km/sec，2.4～3.2 km/sec，4.7～5.0 km/secである．3地点での地下構造で特徴的なことは，基盤深度が各地点で異なっているにも拘わらず，最上部の最新世層の厚さが約1 kmとほぼ一定していることである．また，基盤岩の速度がP波S波とも，夢の島爆破による屈折波探査結果と有為な違いがあることが見いだされた．このことは，基盤岩の速度異方性による可能性もあるが，基盤岩のコアサンプルの速度測定結果には顕著な異方性は確認できず，2層基盤等の基盤内部の構造の複雑さによる可能性を示唆している．本論での結果と他の孔井の地質柱状図，地震波屈折法探査結果，重力探査結果等を総合して，首都圏下を含む関東平野の基盤の三次元構造の概略を明らかにした．すなわち，基盤は北西領域で約1～1.5 kmとやや浅く，筑波山と銚子に向かってしだいに浅くなり両地点で露出している．西に向かっては，急激に浅くなり関東山地に続いている．深さ3 kmを越える窪みが首都圏の西部を通り南北に連なっている．最深部は横浜の南西方に位置し，約3.7 kmの深さである．

* 先端解析技術研究部　数理解析研究室